AC Losses in High Temperature Superconductors under non –Sinusoidal Conditions

By Spector Marat

B.Sc., Ben-Gurion University, 2007

e-mail: maratspector@gmail.com

Masters Thesis, October, 2010

Submitted in partial fulfillment of the requirements for the degree of Master in Physics in the Faculty of Natural Sciences at Ben-Gurion University of the Negev, Beer-Sheva, Israel

Author signature _____ Date _____

Supervisor approval _____ Date _____

Supervisor approval _____ Date _____

Department Council approval _____ Date _____

Dedicated to my beloved family

Abstract

AC losses in superconductors characterize their physical properties (the microscopic motion of the Abrikosov vortices, phase state of the vortex lattice, etc) as well as determining ranges of the rated currents and magnetic fields for superconducting devices that are required for the optimal operation power of cryogenic equipment and economical gain. The methods of AC loss calculation are usually based on consideration of the non-linear Maxwell equations in which a superconductor is simulated by a media with non-linear voltage current characteristic, in the general case which depends on a local magnetic field and a local temperature. Many investigations are devoted to a consideration of AC losses in superconductors of various forms such as wires, tapes, coated conductors, etc., under different conditions. However, most of the works consider sinusoidal magnetic fields or/and currents. In reality, currents in physical experiments and in electric power systems exhibit a distribution of harmonic frequencies.

The main goal of this thesis is the treatment of AC losses in superconductors and coated conductors under non-sinusoidal conditions.

Analytical expressions were obtained for various configurations of superconductors such as: bulk materials, thin strips, coated conductors in the framework of critical state model as well as in high magnetic field approximation for a power law superconductor. An analysis of losses in power law superconductors was carried out using the MatLab software to perform numerical solution of the integral equation.

The analysis shows that in devices with bulk superconductors, higher harmonics can substantially change losses. Thus, the 5% second harmonic can cause a loss increase of 20% in superconductors in comparison to 1% for a normal metal. Moreover, the contribution of the higher harmonics depends on their phases. In a certain range of phases, the odd harmonics can even reduce AC losses. These peculiarities distinguish the behavior of superconducting devices from that of conventional ones.

Influence of higher harmonics losses in coated conductors is markedly stronger. Thus, the 5% third current harmonic causes a loss increase of 45% in the superconducting part of a coated conductor and 80% in the normal-metal parts at a current close to the critical value.

Numerical calculations of the total losses (sum of losses in superconducting and normal metal parts) in a coated conductor within the power-law approximation showed that the relative contribution of higher harmonics increases with their amplitude.

The relative contribution of the third 10% harmonic to the total losses can achieve up to 110% of the losses caused by the main harmonic and is about ten times larger than losses caused by the same higher harmonic in the normal-metal conductor of the same form. Even at a low power index (n = 4) the predicted losses are substantially higher than AC losses in normal metals: relative contribution can be 4 times higher and achieves it 44% of the main harmonic losses replace of 11%.

Acknowledgements

The author wishes to thank Dr. Vladimir Sokolovsky for his extraordinary patience close guidance, support and teaching in the theory of superconductivity and the solid state physics of superconducting materials. The world of superconductivity would not be accessible to me without him.

To Prof. Shuker Reuven for the unique teaching and guidance, using his knowledge and experience in many areas of physics. His unique knowledge alleviated my understanding.

To Prof. Leonid Prigozhin for his important teaching in theory, and his important help in the numerical analysis and simulation of power law superconductors.

To Dr Victor Meerovich for his assistance and help.

Content

1. Introduction

A superconductor has zero resistance only under DC conditions, under AC conditions a changing magnetic field (either self generated or externally applied) acting on the material interacts with transport and leads to energy dissipation. The subject of AC losses in superconductors may be considered under various aspects.

Firstly, the physical properties of high temperature superconductors (HTSC) such as: the microscopic motion of Abrikosov vortices, phase state of the vortex lattice, current density, critical temperature and also with developing the theory where the microscopic processes are described by a nonlinear current –voltage characteristic $\vec{E} = \vec{E}\left(\vec{J}, \vec{B} \right)$ (E is the local electric field caused by the current density J and depending also on a local magnetic induction B) and by reversible magnetization curve $\vec{H} = H\left(\vec{B} \right)$ [1-3] .

Secondly, from the technical point of view AC loss values determine ranges of the rated currents and magnetic fields for superconducting devices, required power of cryogenic equipment and economical gain.

The methods of AC loss calculation are usually based on consideration of the non-linear Maxwell equations in which a superconductor is simulated by a metal with non-linear voltage current characteristic, in the general case, depending on a local magnetic field and a local temperature.

A lot of investigations are devoted to a consideration of AC losses in superconductors of various forms, wires, tapes, coated conductors and. under different conditions (see for example [4-6] and works referenced in them). However, most of the works consider sinusoidal magnetic fields or/and currents. In reality, currents $I(t)$ in physical experiments and electric power systems contain a wide variety of harmonics and can be represented as

$$I(t)=\sum_k I_k \cos\left(k\omega t+\phi_k\right) \tag{1.1}$$

where $\omega=2\pi f$, f is the frequency of the first harmonic, I_k and ϕ_k are the amplitude and phase of the *k*-th harmonic, (*k* = 0,1,2…..). The frequency f for power systems is 50 or 60 Hz, while for special electric systems (airplanes, ships, etc.) frequently is 400-800 Hz.

For the normal metal parts of a device the Joule losses P_j caused by a current $I(t)$ and the eddy losses P_{ed} caused by a magnetic field $H(t)$ are presented in the form:

$$\begin{aligned} P_j &= \frac{R(f)I_1^2}{2}\left(1+\sum_{k\neq 1} r_k i_k^2\right) \\ P_{ed} &= \frac{K_1(f)H_1^2}{2}\left(1+\sum_{k\neq 1} p_k h_k^2\right) \end{aligned} \tag{1.2}$$

where $R(f)$ is the conductor resistance at the frequency f, r_k gives the frequency dependence of the resistance, $i_k=\frac{I_k}{I_1}$, $h_k=\frac{H_k}{H_1}$, H_k is the *k*-th harmonic amplitude of the magnetic field, $K_1(f)H_1^2/2$ is the eddy losses caused by the main harmonic, p_k characterize the dependence of the losses on the frequency. The explicit forms of *R*, *K*, r_k ,p_k depend on the conductor shape and magnetic field direction. For example, losses per unit length in a thin normal metal strip in an external magnetic field directed perpendicular to the wide surface are

$$K_1=\frac{2\mu_0^2 a^2 d\omega^2}{3\rho} \text{ and } p_k=k^2 \tag{1.3}$$

where μ_0 is the magnetic permeability of the vacuum, ρ is the resistivity, d is the strip thickness, a is a half of the strip width.

According to the requirements of power quality supported by power systems, the contribution of higher harmonics is a few percent and currents are very close to sinusoidal. Usually higher harmonics decrease proportionally to $\frac{1}{k}$ at least and it is sufficient to take into account

several first harmonics. $I_0 = 0$ because a direct current cannot be transferred by the transformer. So, with the accuracy of about 1% the losses in normal conducting parts of the power devices are determined by the main harmonic. Currents become strongly non-sinusoidal at the operation of the converters, non-linear reactors and during transient and overload conditions. In this case all harmonics have to be taken into account at the loss estimation. Since superconductors posses a strongly non-linear current voltage characteristic, one can expect substantial contribution of higher harmonics to AC losses in superconducting elements.

The main goal of this thesis is the consideration of AC losses in superconductors and coated conductors under non-sinusoidal conditions.

The objectives are the following

- analysis of penetration of a non-sinusoidal magnetic field into superconducting slab, thin film (strip), and coated conductor;
- development of analytical methods for AC loss calculation based on the critical state model (CSM);
- numerical calculation of AC losses in power law superconductors and coated conductors.

The thesis structure is the following:

Chapter 2- contains a brief introduction to the subject of AC losses in superconductors including description of the mechanism of AC losses, analytical methods for calculation of AC losses in magnetic fields or with transport currents;

Chapter 3- reveals an analytical analysis of AC losses under non-sinusoidal conditions for superconducting slab and thin film (strip);

Chapter 4- represents analytical approach for calculation of AC losses in coated conductors under non-sinusoidal conditions;

Chapter 5- represents results of numerical simulation of AC losses based on the power law approximation for coating conductors.

The main obtained results have been presented in the following papers:

1. V.Sokolovsky, V.Meerovich, **M.Spector**, G.Levin, and I, Vajda
   Losses in superconductors under non-sinusoidal currents and magnetic fields,
   IEEE Trans . Appl. Supercon., v.19 pp: 3344-3347 (2009)

2. G.Furman, **M.Spector,** V.Meerovich, and V.Sokolovsky
   Losses in coated conductors under non-sinusoidal currents and magnetic fields,
   in print in Journal of Superconductivity and Novel Magnetism

and at the conferences

1. V. Sokolovsky, V. Meerovich, **M. Spector**, G. Levin, and I, Vajda,
   Losses in superconductors under non-sinusoidal currents and magnetic fields,
   Applied Superconductivity Conference 2008, August 17-22, Hyatt Regency Chicago, Illinois, Chicago USA, Conference Program p 80, (2MPB09). Poster Presentation

2. G. Furman, **M. Spector,** V. Meerovich, and V. Sokolovsky
   Losses in coated conductors under non-sinusoidal currents and magnetic fields,
   International Conference on Superconductivity and Magnetism 25-30 April 2010, Antalya, Turkey, Abstract Book: p776, (LSA-P-002). Poster Presentation

2. AC losses in superconductors under sinusoidal conditions

2.1 Origin of AC Losses in Superconductors

The vortices in a type II superconductor create a lattice of parallel flux lines through the specimen, each carrying a quantum of magnetic flux $\phi_0 = h/2e = 2.07 \cdot 10^{-15}$ T·m^2 (where h is the Planck constant and e is the electron charge). The magnetic flux penetrates into the specimen through the vortex core, which is in the normal state and located in the centre of the vortex. The magnetic field is maximum near the center and exponentially decays with the distance from the centre over the London penetration depth of the order of 10^{-7} m. The core radius is of the order of coherence length ξ of 10^{-8} m. The density of the vortices in the lattice is determined by a local magnetic field B as $n = \frac{B}{\phi_0}$. This mixed state is observed in the superconductors up to the upper critical magnetic field B_{c2}. The upper critical magnetic field is of the order of 20 T for low temperature superconductors and 100-200 T for high temperature superconductors at 4 K.

The vortices can move freely in a homogenous material, their density is proportional to the flux density and they can be pinned by inhomogeneities in the material. Any motion of vortices results in energy dissipation.

Let us assume that the current is applied in the presence of a magnetic field. In homogenous superconductors the vortices start to move under the influence of the Lorenz force: $\vec{f}_L = \vec{j} \times \vec{\phi}_0$ (j *is* the current density), or per unit of volume of the lattice $\vec{F}_L = \vec{j} \times \vec{B}$. As a result the moving magnetic flux generates an electric field $\vec{E} = \vec{v} \times \vec{B}$ (Fig.1). The motion of vortices results in the energy loss per unit of volume of the lattice $P = J \cdot E$. This motion can be presented as motion opposite the viscous drag force density $f_d = -\eta v$ (η is the viscosity coefficient of the flux lines, v is the velocity of the vortices). In reality superconductors do

contain defects and interaction of vortices with the defects (pinning force) prevents the movement of the vortices until the Lorenz force exceeds the pinning force. There is a current density j_c, the critical current density at which the Lorentz force is equal to the pinning one $f_p = f_L = j_c\phi_0$. At higher currents we observe the vortex motion which is known as "flux flow". The vortex velocity is determined from the equality of the Lorentz force and a sum of the pinning and viscous drag forces. The power loss per unit of volume is proportional to the vortex density n and determined as:

$$p = -f_L v n = J\phi_0^2 n(J - J_c) = \rho_{FF} J(J - J_c) \tag{2.1}$$

where $\rho_{FF} = (\phi_0 B/\eta)$ is the flux flow resistivity depending on a local magnetic field and temperature.

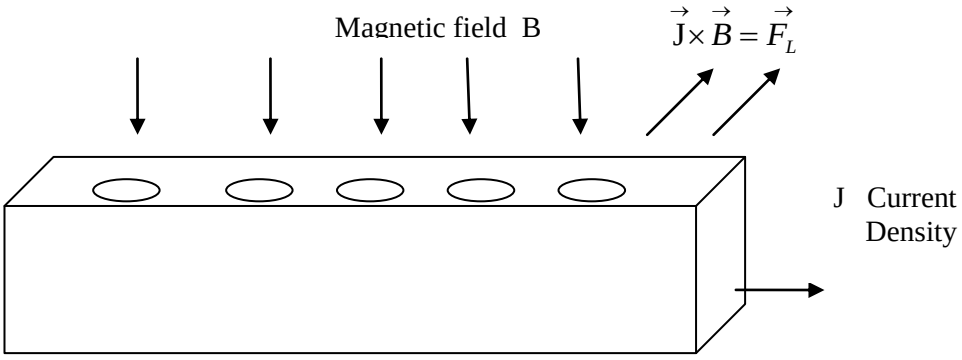

Fig. 1 A superconductor with a current in an external magnetic field

It was shown by Bardeen and Stephen [11] that the expression for ρ_{FF} can be given approximately as:

$$\rho_{FF}(B,T) \approx B\rho_n(T)/B_{c2}(T) \tag{2.2}$$

where ρ_n is the resisitivity in the normal state at temperature T.

The viscosity coefficient can be approximated by:

$$\eta = \phi B_{c2} / \rho_n \tag{2.3}$$

As a result the current density can be presented in superconductors in the form:

$$J = J_c + E / \rho_{FF} \tag{2.4}$$

where the current density J_c flows without dissipation, and an additional part $\delta J = E / \rho_{FF}$ is related to the motion of the electrons of the normal conductivity.

Another mechanism of AC losses predicted by Anderson is the electric field generation in superconductors connected with the thermally activated flux jumps out of pinning centres over the pinning barrier ("flux creep" [7]). A usual method of the flux creep study is based on the measurement of a magnetic field penetration in a hollow superconducting cylinder (decay of persistent current in the cylinder). The decay of the cylinder current in the flux creep regime is usually described by the logarithmic law while the current decay in the flux flow regime obeys to an exponential law. This difference allows one to separate these regimes experimentally.

There are two mechanisms of energy dissipation as a result of the motion of vortices [8,9]:

- moving vortices cross the current lines (due to continuity of the later). Hence a current flows through a vortex parts (vortex cores) which are in the normal state. This leads to energy dissipation.
- when a vortex passes through some point of the superconductor a phase transition occurs in this point from the superconducting to normal state and vice versa. From thermodynamics it is known that such a process can occur without energy dissipation only if a cyclic phase transition is infinitely slow. A velocity of vortex filaments is finite and the phase transition caused by the vortex motion leads to dissipation of energy.

Estimations [10,11] showed that contributions of these loss mechanisms are about the same.

Let us discuss briefly models for analytical calculation of AC losses in superconductors and their range of application.

2.2 Critical State Model

The macroscopic description of magnetic properties type-II low temperature superconductors (LTS) was developed in sixties by C. Bean [12] and is known as the critical state model (CSM). Bean has proposed to use a continuum description of a vortex lattice: a local magnetic field is proportional to vortex density. The conditions when the quantum description could be replaced by the continuum one discussed in many publications and books [for example 13-14]. Brandt noted that a continuum description of a vortex lattice is valid at $B > 2B_{c1}$ [17]. The basic postulate of CSM is that there is a limiting macroscopic superconducting current density J_c that every superconductor can carry without resistance and any electromotive force will induce this current density. This assumption was based on two facts known for LTS. First, the flux creep regime is observed in a very narrow region near J_c. Second the addition of δJ to the critical current density is very small. The following estimations confirm the last point. The LTS are usually used in the form of the multifilament wires where the diameter d of a multifilament is about 10^{-5} m. From the Maxwell equations, the induced electric field in a filament placed in AC magnetic field with the frequency f and amplitude B_0 can be estimated as $E \approx 2\pi fdB_0$. Taking into account Eqs. (2.2) and (2.4), the additional current density is $\delta J \approx \frac{2\pi fdB_{c2}(T)}{\rho_n(T)}$. The upper critical field B_{c2} and normal resistivity ρ_n of LTS are the order of the magnitude of 20 T and $10^{-8}\ \Omega\cdot\mathrm{m}$, correspondingly, and $J_c = 10^{10}$ A/m^2. Therefore, $\delta J / J_c \sim 10^{-3}$ at the frequency of 50 Hz. Thus, in real conditions the additional current density is much less than the critical current density.

The basic points of Bean's model can be summarized as follows:

- current density in a superconductor is equal to J_c or 0;
- critical current density appears whereas there is nonzero electric field;
- current density remains constant with time when an electric field equals to zero;
- current density is field independent;

- magnetic field penetrates a superconductor from its surface .

Note that Bean's model describes magnetic properties of a hard superconductor in a steady-state limit. Since any variation of the magnetic flux in the sample results in an induced electric field, superconductors in the dynamic regime are always in the resistive state (a current density is higher than the critical value). This fact is usually neglected for the analysis of the magnetic properties of LTS's in dynamic regime.

The technique of the AC loss calculation is based on classical electrodynamics (Maxwell's equations):

$$\vec{\nabla}\times\vec{E}=-\frac{\partial\vec{B}}{\partial t};\quad \vec{\nabla}\times\vec{H}=\vec{J};\quad \vec{\nabla}\cdot\vec{D}=0;\quad \vec{\nabla}\cdot\vec{B}=0;\quad \vec{B}=\mu_0\vec{H} \tag{2.5}$$

complemented by Bean's assumptions. Here D is the electric field induction which is proportional to E and the linear relation between B and H is valid only for an isotropic superconductor at $B>2B_{c1}$ [15].

There are various methods for calculation of losses in the superconductor per a period of the current:

- integrating the Poynting vector $\vec{S}=\vec{E}\times\vec{H}_e$ (where H_e is magnetic field at the superconductor surface), on the sample surface over the period;

- integrating the power Joulle losses $E\cdot J_c$ through the sample volume

- calculation of the work of mechanical forces put out opposite the pinning forces at the motion of the vortex lattice. Loss power per unit volume is equal to $p=\left(\vec{J}_c\times\vec{B}\right)\cdot v$, where the velocity v of the vortices can be determined by the conservation law of vortex density $div\left(\left|\vec{B}\right|\vec{v}\right)=\frac{\partial\vec{B}}{\partial t}$.

- using the surface impedance concept. The surface impedance is defined as the relation of the first harmonic of electric and magnetic fields on the surface:

$$Z = \frac{1}{\pi H_0} \int_0^{\pi} E(x=0,t) exp(i\omega t) d(\omega t) \tag{2.6}$$

where *i* is the unit imaginary number.

The loss power *P* dissipated in a sample is determined by the real part of the surface impedance:

$$P = Re(z) H_0^{\,2}$$

This concept is widely used for characterization of superconductors in high magnetic fields.

- calculation using AC susceptibility.

For sinusoidal external magnetic field one may define the complex susceptibility

$$\chi_m = \chi_m' - i\chi_m''; \qquad m = 1,2,3\ldots..;$$

$$\chi_m(H_0,\omega) = \frac{i}{\pi H_0} \int_0^{2\pi} M(t) exp(im\omega t) d(\omega t) \tag{2.7}$$

where $M(t)$ is the component of the (dipolar) magnetic moment of *M* along the external magnetic field. The magnetic moment is

$$M(t) = \frac{1}{2} \int r \times J(r,t) d^3 r \tag{2.8}$$

The energy converted into heat in the whole of the specimen during one cycle of the AC field is proportional to the imaginary part of the first harmonic

$$P = -\pi \chi_1'' \mu_0 H_0^{\,2} \tag{2.9}$$

The real part of the complex AC susceptibility determines the time average of the magnetic energy stored in the volume occupied by the sample. The approach is widely used to describe the linear and nonlinear response of HTSC specimens in various geometries (slab, infinite and finite cylinders, strip, disc, and etc. [16,17]). The AC susceptibility allows one not only to determine value of AC losses but also to conclude the physical properties of the material.

2.2.1 Analytic calculation of AC losses in a superconducting slab

Let us consider a superconducting slab with thickness 2Δ whose inward surface normal points in the positive *x*-direction. The external sinusoidal magnetic field: $H_e = H_0 \sin(\omega t)$ is applied in the *z*-direction, which is parallel to the surface of the slab while the electric field *E* and current *J* are induced along the *y*-axis. Fig. 2 shows two different cases of a distribution of the magnetic field and current in a superconducting slab; the first one (top) relates to the slab placed in a magnetic field while the second case (bottom) corresponds the slab with a transport current.

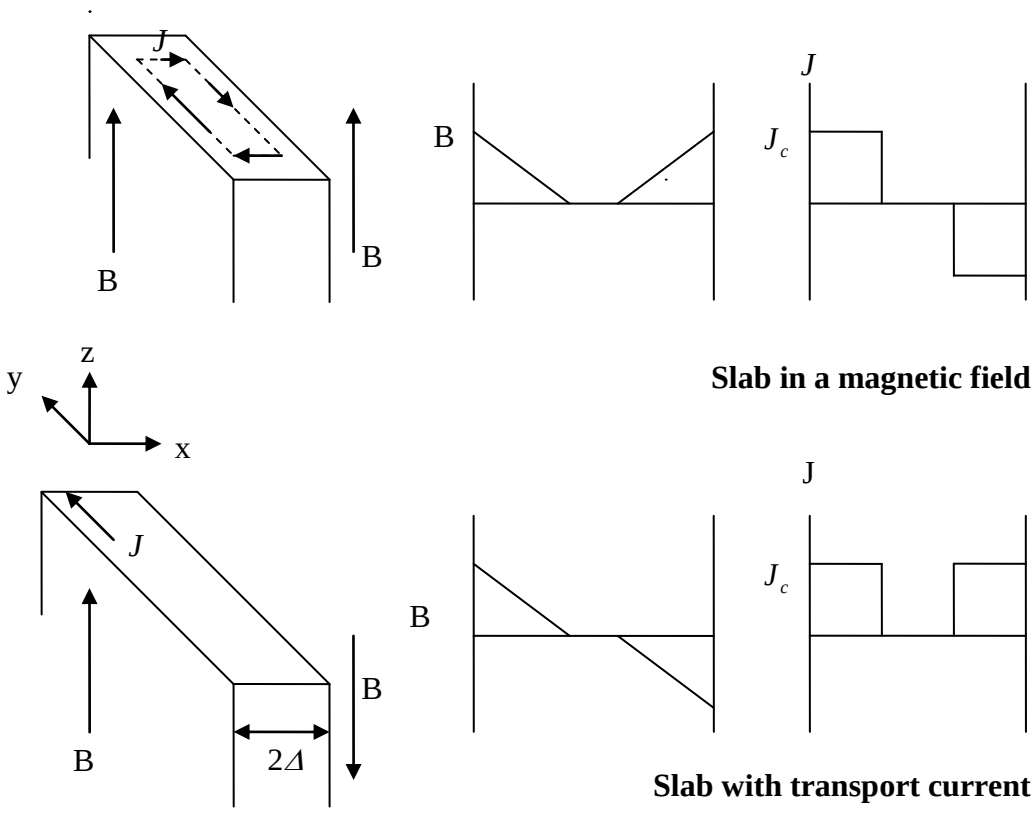

Fig. 2 The profiles of the magnetic field and current in a slab in an external magnetic field (top) and with a transport current (bottom).

The problem is symmetric and hereafter it is sufficient to consider only one half of the slab thickness from $x = 0$ till $x = \Delta$ and one half of the period of the applied magnetic field e.g. between the minimum $H_e = -H_0$ to the maximum $H_e = H_0$. According to the Bean model for the initial state at $\omega t = -\pi/2$ the current density is $J = -J_c$ for all x reached by the

penetrating magnetic field. For the slab, in the area in which magnetic field penetrates, Eqs. (2.5) are reduced to

$$\frac{\partial H}{\partial x} = -J_c \tag{2.10}$$

$$\frac{\partial E}{\partial x} = -\mu_0 \frac{\partial H}{\partial t} \tag{2.11}$$

with boundary conditions: $H = H_e$ at $x = 0$ and $x = 2\Delta$.

This initial profile of the magnetic field is marked as 1 in Fig. 3. In the case of an incomplete penetration (the amplitude of the applied magnetic field H_0 is less than the complete penetration field $H_p = J_c\Delta$) there is a region when magnetic field and current are absent. The region with $J = -J_c$ extends to the Bean penetration depth $x_p = H_0 / J_c$. In the case of the complete penetration, $H_0 \geq H_p$, magnetic field penetrates the whole of the slab and the region with $J = -J_c$ extends to $x_p = \Delta$ (Fig. 3 b).

As the magnetic field increases, the profile of the current density changes and starts to contain a region with $J=J_c$. Let us denote by x_1 the point at which the current reverses its sign. We have $J = J_c$ for $x \leq x_1$ and $J = -J_c$ for $x>x_1$.

The solution of Eq. (2.10) is

$$H = \begin{cases} H_e - J_c x, & x \leq x_1 \\ -H_0 + J_c x, & x > x_1 \end{cases} \tag{2.12}$$

The point x_1 is determined from a continuum for the magnetic field in this point

$$x_1 = (H_e + H_0) / 2J_c \tag{2.13}$$

In this point the electric field equals zero: $E(x_1) = 0$. This is the boundary condition for Eq. (2.11). The electric field in the superconductor is

$$E = \begin{cases} \mu_0 \frac{\partial H_e}{\partial t}(x_1 - x_0), & x < x_1 \\ 0, & x_1 < x < \Delta \end{cases} \tag{2.14}$$

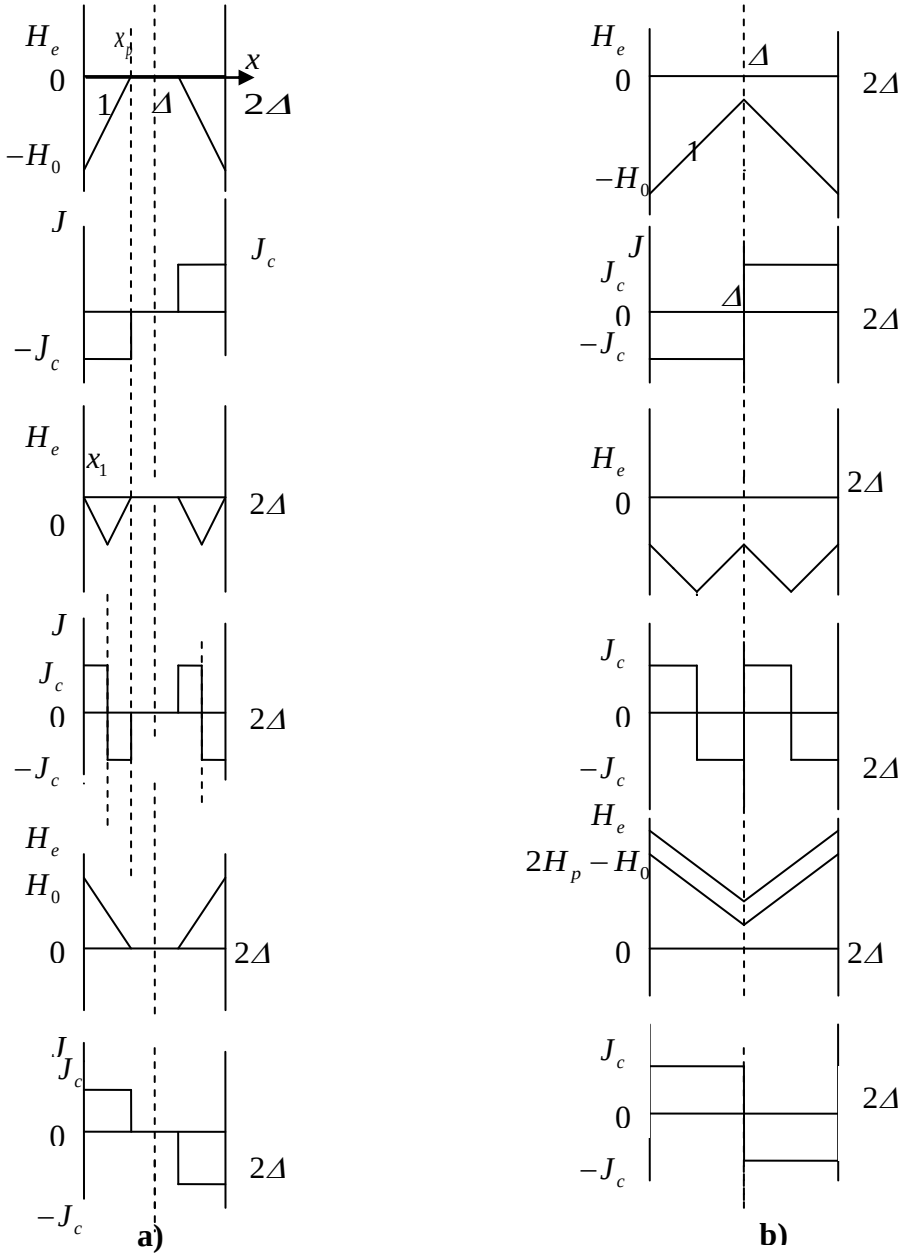

Fig. 3 The profiles of the magnetic field and current in a slab at the increase of external magnetic field from -H_0 to H_0 for the cases of an incomplete penetration (left column) and the complete penetration (right column).

Note that in the case of the complete penetration the increase of an applied magnetic field above $2H_p - H_c$ does not lead to increase of the current density in the superconductor. At the external magnetic field above $2H_p - H_c$, $x_1 = \Delta$, and the boundary condition for the Eq. (2.11) is zero electric field in the centre of the slab. There are several different approaches for

calculation of AC losses per a period of time in a superconductor. Here we will use the formula for the power Joule losses, i.e. by integrating $E \cdot J_c$ through the sample volume and period. The calculation procedure is in details presented in many papers (see for example [2,12]), here we represent the results for the case when a superconducting slab and an infinitely long cylinder are subjected to a sinusoidal external field or a transport current. For the case of the incomplete penetration $H_0 < H_p$, the loss density per a period and per a surface unit is determined as

per one side of a slab: $p = \frac{2\mu_0}{3J_c} H_0^{\,3}$; (2.15)

for a cylinder: $p = \frac{2\mu_0}{3J_c} H_0^{\,3}(1-\frac{H_0}{2J_cR})$; (2.16)

for the case of complete penetration:

for one side of a slab: $p = \frac{2\mu_0 H_p^2}{J_c}(H_0 - \frac{2}{3}H_p)$; (2.17)

for a cylinder:

$$p = \frac{2\mu_0 H_{pc}^2}{J_c}(H_0 - \frac{2}{3}H_{pc})\left(1-\frac{2H_0 - \frac{3}{2}H_{pc}}{3H_0 - 2H_{pc}}\right); \quad (2.18)$$

where for the cylinder $H_{pc} = J_c R$, R is the radius of the cylinder.

Total power losses are determined by multiplying Eqs. (2.16)-(2.18) by the sample surface and frequency. Losses in the slab with the alternating transport current can be determined using equation (2.12) where the magnetic field amplitude H_0 is replaced by the $I_0/2$ (where I_0 is the amplitude of the current per a height unit of the slab). AC losses per a period per unit of length of the superconducting cylinder with a transport current along its axis are:

$$p = \pi\mu_0 J_c R^4\{(1-i)[\ln(1-i)+i]+\frac{i^2}{2}\} \quad (2.19)$$

where $i = \frac{I_a}{I_c}$; I_a is the amplitude of transport current; $I_c = J_c \pi R^2$ is the critical current of the cylinder.

2.3 AC losses in thin superconducting strip

In the previous section we considered AC losses in bulk superconductors using the model of an infinitely long slab (cylinder) with a transport current or in an external magnetic field parallel to the superconductor surface. In many cases of real applications superconductors, such as thin films, tapes, coated conductors, can be simulated by infinitely long thin strips carrying a transport current or in an external magnetic field [4, 17, 18]. Below we will briefly discuss the main points of the mathematical model developed in [17,18] for analysis of magnetization and AC losses in the strips. Let us consider a superconducting strip filling the space $|x| \le d/2$, $|y| \le a$, $|z| < \infty$ with $d << a$ (Fig. 4) and assume that the critical current density j_c is independent of a local magnetic field. Taking into account that $d << a$ consideration of a real current distribution in the strip cross-section is reduced to consideration of a sheet current determined as [4,17]:

$$J(y) = \int_{-d/2}^{d/2} j(x,y)dx .$$

In the frame of this approximation the *y*-component of a magnetic field on the superconductor surface is $H_y(d/2, y) = -\frac{1}{2}J(y)$ (upper surface, $y > 0$) and $H_y(-d/2, y) = \frac{1}{2}J(y)$ (lower surface, $y < 0$) and the *x*-component $H_x(d/2, y) = H_x(-d/2, y) = H(y)$ and is given by [4,17]:

$$H(y) = \frac{1}{2\pi}\int_{-a}^{a} \frac{J(u)du}{y-u} + H_e \ . \qquad (2.20)$$

The magnetic field penetrates through the superconducting strip only in the area, where $J = J_c = \int_{-d/2}^{d/2} j_c dx$. Where $J < J_c$ the x-component of the magnetic field is zero at.

The current distribution is sought in the form: $J = \pm J_c$ near the strip ends and as a solution of Eq. (2.20) with $H(y) = 0$ in a central part of the strip.

The negative magnetic moment M and the total magnetic flux Φ per length unit of the strip are defined by

$$M = \int_{-a}^{a} yJ(y)dy \tag{2.21}$$

$$\Phi = \mu_0 \int_{-a}^{a} H(y)dy = \mu_0 \left(2aH_e + \frac{1}{2\pi} \int_{-a}^{a} J(u) \ln \left| \frac{a-u}{a+u} \right| du \right). \tag{2.22}$$

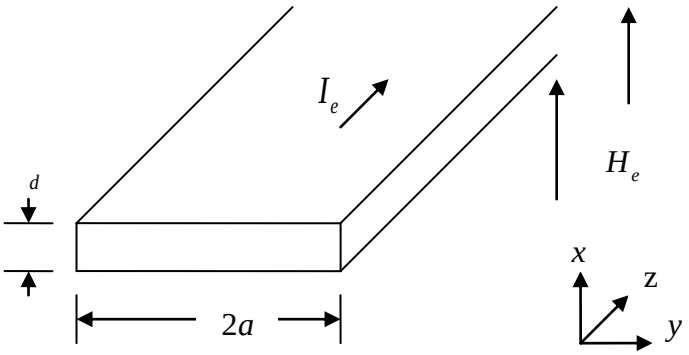

Fig. 4 Strip carrying a transport current in an external magnetic field H_e.

2.3.1 Strip with transport current

In this section we consider a case when a superconducting strip carries a transport current I_t in zero external magnetic field. A sheet current density distribution, as a solution of Eq. (2.20), is given by the following expression [17]:

$$J(y)=\begin{cases}\dfrac{2J_c}{\pi}\arctan\left(\dfrac{a^2-b_I^2}{b_I^2-y^2}\right)^{1/2}, & |y|<b_I \\ J_c, & b_I<|y|<a\end{cases}. \tag{2.23}$$

Integrating this one gets the total current (transport current)

$$I_t = 2J_c\left(a^2-b_I{}^2\right)^{1/2} \tag{2.24}$$

and the penetration width $b_I = a\left(1-\left(I_t/I_c\right)^2\right)^{1/2}$ (2.25)

where $I_c = 2aJ_c$ is the maximum critical current occurring at full penetration $b_I = 0$. We may obtain the magnetic field profiles by using Ampere's law and Eq. (2.23) [4].

$$H(y)=\begin{cases}0 & , \quad |y|<b_I \\ \dfrac{H_c y}{|y|}\operatorname{arctanh}\left[\dfrac{y^2-b_I^2}{a^2-b_I^2}\right]^{1/2} & , \quad b_I<|y|<a \\ \dfrac{H_c y}{|y|}\operatorname{arctanh}\left[\dfrac{a^2-b_I^2}{y^2-b_I^2}\right]^{1/2} & , \quad |y|>a\end{cases} \tag{2.26}$$

where $H_c = J_c/\pi$.

The results (2.23)-(2.26) apply to the initial virgin state where I_t is increased from zero. The corresponding expressions for an alternating applied current with amplitude I_1 are obtained by looking e.g., at the situation when I_t is reduced monotonically from I_1 to - I_1. We can see that the resulting current $J_\downarrow$ and field $H_\downarrow$ profiles are linear superpositions of the form [17]

$$\begin{aligned}J_\downarrow(y,I_e,J_c) &= J(y,I_1,J_c)-J(y,I_1-I_e,2J_c)\\ H_\downarrow(y,I_e,J_c) &= H(y,I_1,J_c)-H(y,I_1-I_e,2J_c)\end{aligned} \tag{2.27}$$

with $J(y,I_e,J_c)$ and $H(y,I_e,J_c)$ given by Eqs. (2.23) and Eqs. (2.26).

When $I_e = -I_1$ is reached, the original state is reestablished, with *J* and *H* having changed sign, $J(y,-I_1,J_c) = -J(y,I_1,J_c)$ and $H(y,-I_1,J_c) = -H(y,I_1,J_c)$. In the half period with increasing I_e one has $J_\uparrow(y,I_e,J_c) = -J_\downarrow(y,-I_e,J_c)$ and $H_\uparrow(y,I_e,J_c) = -H_\downarrow(y,-I_e,J_c)$.

When I_e increases from $-I_1$ to I_1 the electric field in the strip is $E(y) = \frac{\partial \Phi(y)}{\partial t}$ with the magnetic flux $\Phi(y) = \mu_0 \int_o^y H(u)du$. The energy dissipated in the strip during this half cycle is then

$$U_{HC} = \int_0^{\pi/\omega} dt \int_{-a}^{a} E(y)J(y)dy = 2\mu_0 J_c \int_{b_I}^{a} dy \int_b^y H(u)du . \tag{2.28}$$

Inserting (2.26) in (2.28) and performing integration one obtains the dissipated power $P=2fU_{HC}$ per length unit of the strip [17]:

$$P = \left(f\mu_0 I_c^2\right) q\left(I_1 / I_c\right) \tag{2.29}$$

where $q(x) = (1-x)\ln(1-x) + (1+x)\ln(1+x) - x^2$.

For small and large amplitudes this gives

$$P = \begin{cases} \left(f\mu_0 / 6\pi I_c^2\right) I_1^4 , & I_1 << I_c \\ \left(f\mu_0 / \pi\right)(2\ln 2 - 1) I_1^2 , & I_1 = I_c \end{cases} \tag{2.30}$$

2.3.2 Strip in a perpendicular magnetic field

The current and field profiles in a thin strip in a perpendicular field H_e and with zero transport current can be calculated in a similar way as for the current carrying strip in Sec 2.3.1. Here we present the results for current and magnetic field profiles for a thin strip in a perpendicular field [17]:

$$J(y)=\begin{cases}\dfrac{2J_c}{\pi}\arctan\left[\dfrac{c_H y}{\left(b_H{}^2-y^2\right)^{1/2}}\right], & |y|<b_H \\ J_c y/|y|, & b_H<|y|<a\end{cases} \tag{2.31}$$

$$H(y)=\begin{cases}0, & |y|<b_H \\ H_c\operatorname{arctanh}\dfrac{\left(y^2-b_H{}^2\right)^{1/2}}{c_H|y|}, & b_H<|y|<a \\ H_c\operatorname{arctanh}\dfrac{c_H|y|}{\left(y^2-b_H{}^2\right)^{1/2}}, & |y|>a\end{cases} \tag{2.32}$$

where $b_H=a/\cosh\left(H_e/H_c\right)$, $c_H=\tanh\left(H_e/H_c\right)$. The results (2.31)-(2.32) apply to the initial virgin state where H_e is increased from zero.

At the end one can obtain in a similar way as described in Sec 2.3.1 the expression for the dissipated power when the strip is in an external sinusoidal magnetic field [17]

$$P=4f\mu_0 a^2 J_c H_1 g\left(\frac{H_1}{H_c}\right)$$
$$\text{where } g(x)=\frac{2}{x}\ln\left(\cosh(x)\right)-\tanh(x). \tag{2.33}$$

For small and large amplitudes H_1 this gives

$$\begin{aligned}&P=\left(2\pi\mu_0 a^2/3H_c^2\right)H_1^4, && H_1<<H_c \\ &P\approx 4f\mu_0 a^2 J_c\left(H_1-H_c\right) && H_1>>H_c\end{aligned}. \tag{2.34}$$

2.4 Further development of Bean's Model

Bean's critical model has been successfully applied for the calculation of AC losses and analysis of magnetic behaviour of low temperature type-II superconductors and gives a good agreement with experimental data. For high magnetic fields deviations between the experimental data and the prediction given by this model have been found.

One of the main reasons for these deviations is the dependence of the critical current density on a local magnetic field. This dependence is particularly strong for HTSCs and manifests itself even for low magnetic fields.

The development of the Bean model was directed towards consideration of the magnetic field dependence of the critical current density. One of the widely used models is the Kim-Anderson model [19]:

$$j = \frac{j_0}{1 + H / H_{con}} \tag{2.35}$$

where j_0 and H_{con} are the constants of the material.

Other widely used models are

$J = J_C (H_{c1} / H)^n$, Yeshurun [20]

$J_C = J_0 \exp(-H / H_{con})$, Fietz [21]

$J_c = J_0 / (1 + H / H_{con})$, Watson and Shi [22]

$J_c = K / H^{1/2}$, Matshushita [23].

The fitting parameters of the models j_o, H_{con}, H_{c1}, K can be determined experimentally from the critical current measurements in DC magnetic field, from experimental investigation of the dependence of the AC losses and susceptibility on the magnetic field [16], and of the magnetic shielding properties of superconductors [24].

In the framework of the models listed above, the Bean dependencies of the losses on the magnetic field amplitude are disturbed. Note, however, that the losses per a period are frequency independent as it is given by the original Bean model.

2.5 Losses in HTSC

After the discovery of high temperature superconductivity the Bean model and the other models based on the conception of the critical state are used for the description of the magnetic field

response of new class superconductors [25]. It is noted in many papers the CSM gives the good agreement with experimental data.

However, pronounced deviations from CSM predictions are observed in many experiments. In particular, the penetration threshold of magnetic field depends on the rate of magnetic field increase.

A pronounced frequency dependence of AC losses per cycle in HTSC materials was found [26]. It was noted that an HTSC sample demonstrated pronounced deviations from the CSM under varying external conditions.

2.5.1 Peculiarities of HTSC

HTSC have clearly defined the granular and the layered structure and hence, these superconductors are highly anisotropic. The granularity is caused by weak links at grain boundaries. These links have a very low J_c as compared with granules and magnetic field penetrates to the centre of the sample leaving the grains unpenetrated.

Other peculiarities of HTSC are associated with particular properties of the vortex lattice described in reviews [15,25]. It is noted that the oxidant vacations in HTSC can be the pinning materials. These pinning centres posses a lower potential barrier than defects of the material structure. It reduces the critical current density and increases the effect of flux creep. In HTSC the thermal depinning is observed in wide temperature and current intervals below the critical values. A strong and rapid flux creep, i.e. the thermally activated motion of vortices, is the characteristic feature of HTSC. This "giant flux creep" [20] can be observed till very high electric fields $\approx 10^{-3}$ V/cm in comparison with LTSC where the creep is observed only at electric fields of the order of 10^{-6} V/cm and in a very narrow range of current near the critical value. The criterion of 1 μV/cm for the critical current of a LTS clearly determining the demarcation line between the flux creep and flux flow regimes loses

its meaning in HTSC. For HTSC, the transition point from one regime to the other depends on the superconductor type, preparation technology and external magnetic field.

The thermally activated flux creep leads to a marked decay of persistent currents in the HTSC sample and decreases the magnetization and the gradient of the magnetic field in the superconductor. In LTSC the decrease of the magnetization is well described by logarithmic law [26]. For HTSC, the law of the decrease is dependent on the state of the vortex lattice [27]. In many cases the law is also close to the logarithmic one [20,27]. Formally, this flux creep is equivalent to a nonlinear current –dependent resistivity $\rho \sim exp\left(J / J_1\right)$.

A novel feature in HTSC is the (TAFF) thermally assisted flux flow with a linear (ohmic) resistivity that is observed practically from zero current [28]. The both, flux creep and TAFF are limiting cases of Anderson's general expressions for the electric field $E\left(H,T,J\right)$ which may be written as [9]:

$$E = 2\rho_c J_c \, exp\left(-U_0 / k_B T\right) sinh\left(JU_0 / J_c k_B T\right), \qquad J \le J_c \tag{2.36}$$

where $\rho_c\left(H,T\right)$ is the resistivity at $J = J_c$; $U_0\left(H,T\right)$ is the pinning potential; k_B is the Boltzman constant.

The electric field in HTSC appears from motion of the vortices. At a current density lower than the critical value, the average vortex velocity is determined by the probability of the directional jump of the vortices through a potential barrier. This velocity is determined as

$$v = v_0\left(j / j_c\right) exp\left(-U\left(J\right) / k_B T\right) \tag{2.37}$$

where v_0 is constant ; $U\left(J\right)$ is the activation energy. The $E - J$ characteristic of a superconductor is determined by the substitution of (2.37) in the expression $E = \mu_0 H v$. Generally the activation energy depends on the temperature, magnetic field, vortex lattice state, and pinning type. For LTSC, the usual expression for the activation energy follows from the Kim-Anderson model [7,19].

For HTSC, there are a number of different models confirmed experimentally for different samples. One of the widely used models proposes

$$U(J)=\frac{U_0}{\mu}\cdot\left(\left(\frac{J}{J_c}\right)^{\mu}-1\right) \tag{2.38}$$

Where the exponent μ characterizes the vortex pinning model: single vortex, vortex glass or collective creep models. The parameter μ depends on the properties of HTSC, the external magnetic field and also on the current density and temperature. In the framework of the Kim-Anderson theory $\mu=-1$ and the activation energy is:

$$U(J)=U_0\cdot\left(1-\left(\frac{J_c}{J}\right)\right). \tag{2.39}$$

Theoretical treatment of the collective pinning showed that there are three different regimes depending on the current density J [30]:

$$\begin{aligned}&\mu=7/9, \quad j\ll j_c;\\ &\mu=3/2, \quad j<j_c;\\ &\mu\sim 1, \quad j\sim j_c.\end{aligned} \tag{2.40}$$

Other frequently used forms for the dependence of the activation energy on the current density are the power law $U(J)=U_0\cdot\left(\left(\frac{J}{J_c}\right)^{\mu}\right)$ and the logarithmic law $U(J)=U_0\,ln\left(\left(\frac{J}{J_c}\right)\right)$. The last dependence leads to a power law $E-J$ characteristic in the flux creep region:

$$E=E_0\cdot\left(\frac{J}{J_c}\right)^{n} \tag{2.41}$$

where $n=\frac{U_0}{k_BT}+1$.

Expression (2.41) is frequently used for approximation of a measured *E-J* dependence in the flux creep regime *n* and E_0 are determined from fitting experimental data and for an analysis of magnetic properties and calculation of AC losses in HTSC [6]. Calculation of AC losses is based on numerical methods or approximately approaches [37].

All the models listed above have been applied for calculation of AC losses in superconductors under sinusoidal conditions (sinusoidal magnetic fields or/and currents). In reality, currents $I(t)$ in electric power systems contain a wide variety of harmonics and can be represented by Eq (1.1). Since superconductors posses a strongly non-linear current voltage characteristic, one can expect substantial contribution of higher harmonics to AC losses in superconducting elements. In the next sections we will consider AC losses in superconductors under non-sinusoidal conditions. We are going to take into account the first two harmonics $k = 2$ or $k = 3$. The second harmonic is the main one appearing in two-phase circuits and the third – for three-phase circuits. Usually higher harmonics rapidly decay.

3. Analytical calculation of AC losses in superconducting slab under non-sinusoidal conditions

The waveforms of non-sinusoidal currents (magnetic fields) can be divided into three types: I-symmetrical case a current monotonically increases (decreases) from the minimum (maximum) to the maximum (minimum) and the maximum equals the module of the minimum (Fig. 5, line 1); II –asymmetrical case a current monotonically increases (decreases) from the minimum (maximum) to the maximum (minimum) and the maximum does not equals the module of the minimum (Fig. 5 , line 2); III – a current change is no-monotonic from the minimum to the maximum (Fig. 5, line 3). The type of the waveform depends on the number of harmonics, their frequencies, amplitudes and phases. If $H_e(t) = H_1 cos(\omega_1 t) + H_k cos(k\omega t)$ the monotonic behavior is observed at $\frac{H_k}{H_1} \le \frac{1}{k^2}$.

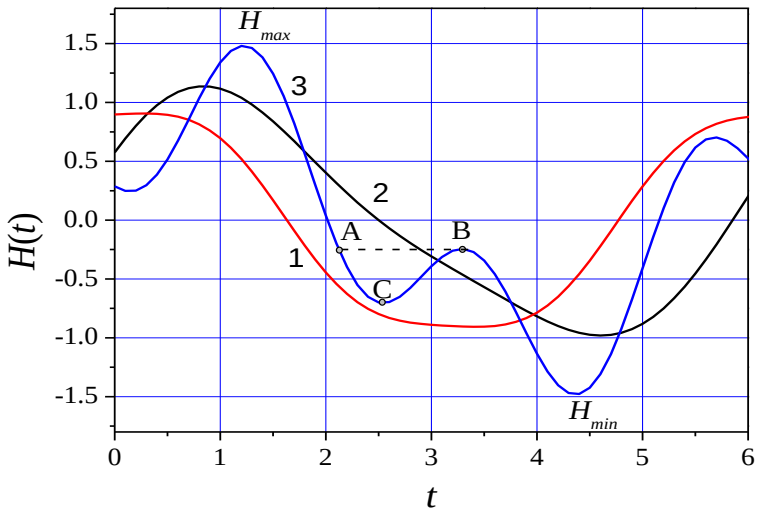

Fig. 5 Non-sinusoidal current waveform: 1 – symmetrical case; 2 - asymmetrical case; 3 - non-monotonic case.

In previous chapter we presented the expressions for calculation of AC losses in the frame of CSM in the cases of sinusoidal external magnetic field or transport current. Using the same approach and mathematical models developed in [8,9,13] we obtained the following

expressions for the AC power losses for non- sinusoidal monotonic current waveforms (symmetrical and asymmetrical cases):

(a) losses per surface unit of a slab in a parallel magnetic field are

$$P=\begin{cases}\mu_0 f\dfrac{\left(H_{max}-H_{min}\right)^3}{6j_c}, & \left|H_{max}-H_{min}\right|<2H_p\\ 2\mu_0 f\dfrac{H_p^2\left(H_{max}-H_{min}-\dfrac{4}{3}H_p\right)}{j_c}, & \left|H_{max}-H_{min}\right|\geq 2H_p\end{cases} \tag{3.1}$$

(b) losses per length unit of a thin strip in a perpendicular magnetic field are

$$P=4\mu_0 a^2 f J_c H_c \Delta h g\left(\Delta h\right), \tag{3.2}$$

where $\Delta h=\dfrac{H_{max}-H_{min}}{2H_c}$, $g\left(x\right)$ is given by Eq. (2.33)

(c) losses per length unit of a thin strip with a transport current are

$$P=\frac{\mu_0 f I_c^2}{\pi}q\left(\frac{I_{max}-I_{min}}{2I_c}\right). \tag{3.3}$$

where $q\left(x\right)$ is given by Eq. (2.29)

Note, that AC losses caused by a current in a slab can be estimated using the first equation of (3.1) where values of the magnetic field are replaced by the current per height unit of the slab.

As seen from Eqs. (3.1)-(3.3) the losses in superconductors under non-sinusoidal monotonic current waveforms are independent of frequency of higher harmonics, while in the case of normal metal parts of the device power of the Joule losses and eddy current losses are given by Eqs. (1.2) and both have a very strong dependence on the frequency of the higher harmonics. Losses per a current period in a superconductor are determined only by the difference $H_{max}-H_{min}$ and are independent of frequency of the main harmonic and higher harmonics.

The AC loss calculation accounting the main harmonic only leads to an error determined by the difference $\Delta H=\left(H_{max}-H_{min}\right)-2H_1$.

To a first approximation, the AC losses can be estimated as

$$P \approx P_1\left(1 + K\Delta H / 2H_1\right) \tag{3.4}$$

where P_1 is the AC losses caused by the main harmonic, K is the coefficient depending on the shape of a superconductor and on the value of H_1. So, K = 3 for a slab at $H_{max} - H_{min} < 2H_p$; K = 4 for a strip at $I_{max} - I_{min} << I_c$ or at $H_{max} - H_{min} << H_c$; K=1 for both configurations at high magnetic fields. A relatively low difference $\Delta H / 2H_1$ leads to a noticeable increase of AC losses. For example, losses increase by up to 20% at $\Delta H / 2H_1 = 0.05$. At the same time, in the normal metal, the five percent second harmonic causes the loss increase by 1%. The difference ΔH is determined not only by the harmonic amplitudes but also their phases (Fig. 6).

And what is more this difference can be negative (Fig. 6b), hence the appearance of higher harmonics can reduce AC losses. At design of superconducting power devices, one should calculate AC losses for the worst case when the losses are maximal. For k = 2 the maximum of ΔH is achieved when $\phi_2 = 0$ and increases as $2.4H_2^{1.8}$, for k = 3 the maximum equals $2H_3$ at $\phi_3 = \pi$.

Now, we consider a non-monotonic current change when additional maximums and minimums appear in the waveforms of magnetic field and current (Fig. 5, line 3). The field cyclically changes from point A to point B through point C. The AC losses induced during this cycle can be calculated using Eqs. (3.1)-(3.3) where H_{max} and H_{min} are replaced by H_A and H_C, respectively. The number of wells and their depths, $H_A - H_C$, depend on the number of harmonics, their frequencies, amplitudes and phases. If $H_e(t) = H_1 cos(\omega_1 t) + H_k cos(k\omega t + \phi_k)$, the maximum well number is k-1. The total AC losses per period are a sum of the losses contributed by all cycles. Fig. 7 presents the characteristic values of a two-harmonic waveform for $\phi_2 = \pi / 2$ at k = 2.

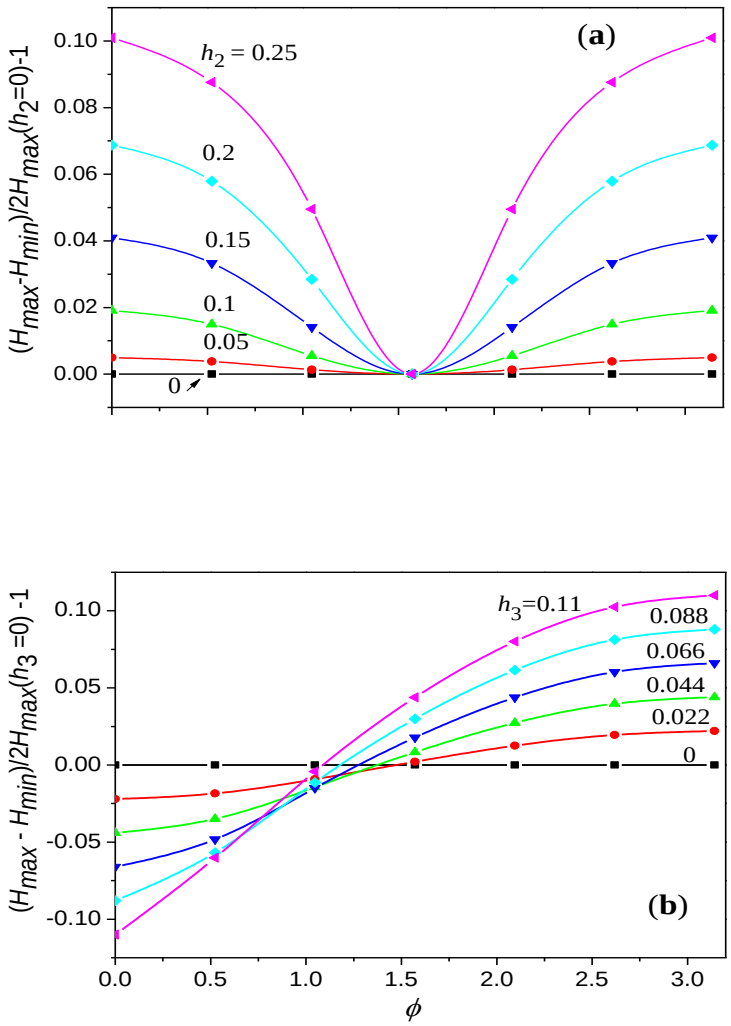

Fig. 6 Dependences of ΔH on phase a) second harmonics b) third harmonics.

At $H_2/H_1 < 0.25$, and $H_{max} - H_{min} = 2H_1$, the losses are determined only by the main harmonic amplitude. If H_2 is higher, the losses increase due to the growth of $H_{max} - H_{min}$ and the contribution of an additional, "inner", cycle. If $H_A - H_C < 2H_p$, the last contribution achieves 5% at $H_2/H_1 = 1$; for $H_A - H_C >> 2H_p$ the 5% level is observed at $H_2/H_1 = 0.4$. So, one has to account the loss part appearing due to wells at relatively high amplitudes of higher harmonics.

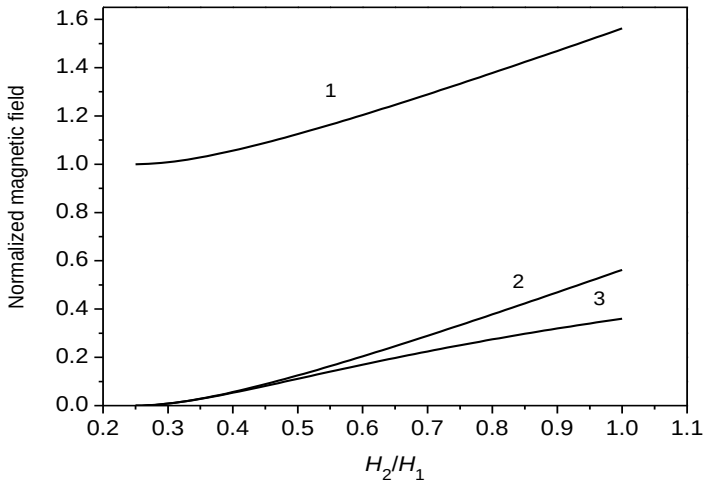

Fig. 7 Normalized characteristic values for $H(t) = H_1 sin(t) + H_2 sin(2\omega t + \pi/2)$ as functions of H_2 / H_1: 1- $(H_{max} - H_{min})/2H_1$; 2 - $(H_A - H_C)/2H_1$; 3 - $(H_A - H_C)/(H_{max} - H_{min})$.

3.1 Summary

The calculation results show that in devices with superconducting elements, higher harmonics can substantially change the loss values. While, in the normal metal, the 5% second harmonic causes the loss increase by 1%, in superconductors this increase can achieve 20%. Moreover, the contribution of the harmonics depends on their phases: in a certain range of phases, the odd harmonics can even reduce AC losses. These peculiarities distinguish the behavior of superconducting devices from that of conventional ones. Non-monotonic character of the waveforms of a current or a magnetic field influences AC losses only at very high amplitudes of additional harmonics.

4. Coated Conductors

In previous chapters we have considered an AC loss problem for the model cases (slab, strip) and shown that existence of higher harmonics can cause pronounced changes of AC losses. For example, the 5% second harmonic can cause the loss increase by 20% in superconductors. Moreover, the contribution of the harmonics depends on their phases: in a certain range of phases, the odd harmonics can even reduce AC losses. These peculiarities distinguish the behavior of superconducting materials from that of conventional ones. In this section we will consider AC losses in the superconducting wire under non-sinusoidal conditions. At present the main candidate for broader commercialization of HTSC wires is the second generation (2G) $YBa_2Cu_3O_{6+x}$ (YBCO)-coated conductor [31,32]. These conductors are produced by deposition of a 1-3 μm film of $YBa_2Cu_3O_{6+x}$ on 10 - 100 μm thick metallic substrate, and superconducting film is subsequently covered by protective silver and stabilizing copper layers (Fig. 10). Buffer layers, typically oxides (CeO_2, MgO, GdZO and etc.), are sandwiched between the YBCO and substrate, the buffer layers are functioned as a texture base, a reaction barrier between the YBCO and the metallic substrate layer and a layer prevents diffusion of metal atoms into the superconductor. The nature of buffer layer is selected depending on the production process of the coated conductor. The typical characteristics of coated conductors are presented in Tabl. 1.

The 2G superconductors are characterized by very high critical current density, up to 4 MA/cm^2 at 77 K, close to that in the epitaxial thin films. The sheet critical current density is usually of the order of 100 A/cm, for the best samples this density can achieve 1000 A/cm [32]. The implementation of superconductors in AC power applications such as transformers, motors and generators depends crucially on the success in designing conductors with low losses in time-varying magnetic environment. AC loss values determine ranges of the rated currents and magnetic fields for superconducting devices, required power of cryogenic equipment, and economical gain. A lot of investigations are devoted to a consideration of AC

losses in coated conductors and coils winded using these conductors under different conditions (see for example [33, 34] and references in them). However, most of the works consider sinusoidal magnetic fields or/and currents.

In this section we will analyze losses in coated conductors under non-sinusoidal conditions when a current monotonically increases (decreases) from the minimum (maximum) to the maximum (minimum) (see Fig. 5, lines 1 and 2).

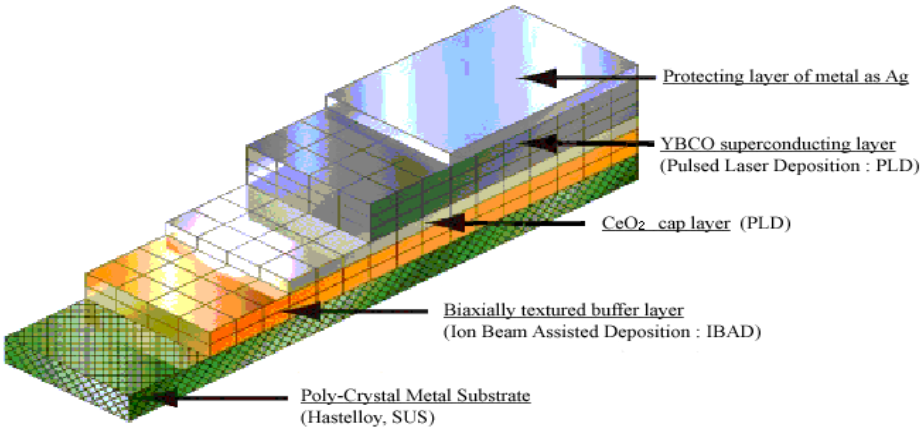

Fig. 10 Sketch of a coated conductor.

Table 1

The typical characteristics of coated conductors

	Thickness of layer	Resistivity at 77 K $\rho\,(n\Omega\cdot m)$
Metal substrate (Ni-alloy)	20-100 μm	4.6
Buffer layer	10-20 nm	dielectric
SC layer (YBCO)	$\leq 5\mu m$	-
Protective layer (Ag)	$25-300\mu m$	2.65
Stabilizer (Cu)	$300\mu m$	2.1

4.1 AC power losses in coated conductor

The total losses in a coated conductor are determined as a sum of losses in a superconductor (hysteresis losses) and in a normal-metal parts (eddy current losses). For loss calculation the coated conductors can be presented as a metal strip and a type II superconducting strip placed one on top of the other as shown in Fig 11. Losses in coated conductors will be calculated for cases: (i) a non-sinusoidal magnetic field is applied perpendicular to the conductor wide surface (in the *z*-direction) and (ii) non-sinusoidal current flows through the conductor in the *y*-direction without an external magnetic field. In this section losses are estimated in the framework of the critical state model neglecting the response of the normal-metal substrate and stabilization layers. For a sinusoidal magnetic field perpendicular to a normal-metal strip the last is valid if

$$\frac{\mu_0 a d_m}{\pi \rho} \omega << 1, \qquad (4.1)$$

where ρ is the resistivity of the metal, d_m and a are the thickness and half-width of the metal strip.

In the mathematical model of a coated conductor the substrate, protective silver and stabilizing copper layers can be represented by an effective normal-metal strip where d_m/ρ is replaced by $d_{sub}/\rho_{sub} + d_{sil}/\rho_{sil} + d_{st}/\rho_{st}$ (here ρ_{sub}, ρ_{sil}, ρ_{st}, and d_{sub}, d_{sil}, d_{st} are the resistivities and thicknesses of the substrate, protective and stabilizing layers, respectively). For a non-sinusoidal magnetic field the condition (4.1) has to be valid for each harmonic taken into account. If the condition (4.1) is valid, the field produced by a current in the normal-metal strip may be neglected and this strip can be considered in a total field which is a sum of the applied field and field produced by a current in the superconductor.

We assume that the normal-metal and superconducting strips are of half-width a and length l and $\{d_{sc}, d_m\} << a << l$. The model of infinitely long thin strips can be applied. In the framework of the thin strip approximation the magnetic field induced by a current in the conductor is perpendicular to the surface and is independent of the *z*-coordinate inside a strip.

The real current distribution through the strip thickness can be replaced by the sheet current determined as an integral of the current density through the strip thickness [4, 17]. Expressions for AC losses in a superconducting strip under non-sinusoidal conditions were obtained in the previous chapter, see Eqs. (3.2) and (3.3). In this chapter we consider eddy current losses in a normal-metal strip and compare them with hysteresis losses. The peculiarity of this consideration is that this strip is subjected to an external non-sinusoidal non-uniform magnetic field.

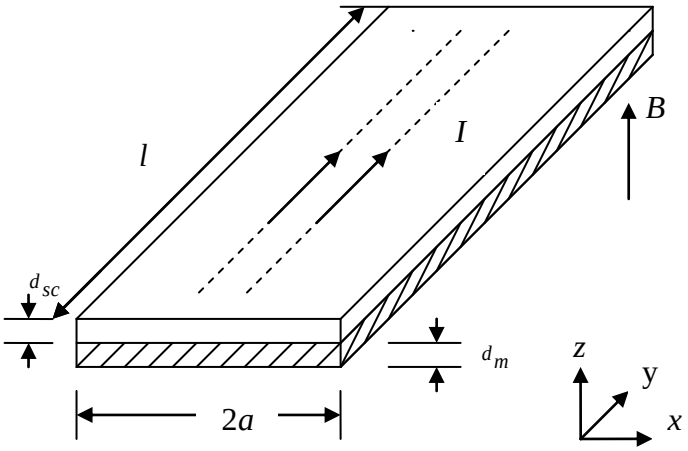

Fig. 11 Sketch of a coated conductor (thin strip approximation), where $d_{sc} < d_m << a << l$, d_{sc} is the superconducting layer thickness

4.1.1 Coated conductor in a perpendicular magnetic field

A non-sinusoidal magnetic field $H_e(t)$ is applied perpendicular to the surface of a coated conductor.

If an external magnetic field monotonically increases, in the framework of CSM AC losses per a period in a superconductor are determined only by the extreme values and do not depend on the waveform and frequency. If the critical current density is independent of a magnetic field, value of these losses is given by Eqs. (3.2). When an external field increases (decreases) the magnetic field is described by the following equations, respectively:

$$H_z = H_z(x,\ H_{\max},\ J_c) - H_z\left(x, H_{\max} - H_e, 2J_c\right) \tag{4.2}$$

$$H_z = H_z(x,\ H_{\min},\ J_c) + H_z\left(x, H_{\min} - H_e, 2J_c\right) \tag{4.3}$$

here, H_z is the *z*-component of the magnetic field which is the sum of the external field H_e and the *z*-component of the magnetic field produced by the currents in the superconducting layer and it is given by, similarly to the case of a sinusoidal external field [33], the following:

$$H_z\left(x, H_e, J_c\right) = \begin{cases} H_c \operatorname{arctanh} \dfrac{\sqrt{x^2 - b^2}}{c|x|}, & b < |x| < a \\ 0, & |x| < b \end{cases} \tag{4.4}$$

where $b = \dfrac{a}{\cosh\left(H_e / H_c\right)}$, $c = \tanh\left(H_e / H_c\right)$, $H_c = J_c/\pi$.

In opposite to a superconducting strip, losses in the normal strip depend on the field extremums as well as on the field waveform. In the considered task there are the y-components of the electric field E_y and current density $j_{y,ed}$, only. The eddy current loss power p_{ed} per unit of volume in an infinity long thin strip is a function of *x* and time *t*:

$$p_{ed} = j_{y,ed}(x,t) E_y(x,t). \tag{4.5}$$

The electric field and current density are related according to Ohm's law:

$$E_y = \rho j_{y,ed}\ . \tag{4.6}$$

The electric field E_y is induced by the time varying magnetic field

$$E_y\left(x,t\right) = -\mu_0 \int_0^x \frac{\partial H_z\left(u,t\right)}{\partial t} du\ . \tag{4.7}$$

The eddy loss power per length unit is:

$$P_{ed} = \mu_0^2 \frac{\omega}{2\pi} \frac{d_m}{\rho} \int_0^{2\pi/\omega} dt \int_{-a}^{a} dx \left[\frac{\partial H_z\left(x,t\right)}{\partial t}\right]^2. \tag{4.8}$$

Integration of the last expression through *x* gives:

$$P_{ed} = \frac{{\mu_0}^2 d_m a^3 \omega^2}{3\pi\rho} H_1^2 F_h \tag{4.9}$$

where

$$F_h = \frac{1}{\omega\pi}\left\{\int_{t_1}^{t_2}\left(\partial h_e\right)^2\left[1-\frac{3}{cosh^2\left(Y\right)}+\frac{2}{cosh^3\left(Y\right)}\right]dt + \int_{t_2}^{2\pi/\omega+t_1}\left(\partial h_e\right)^2\left[1-\frac{3}{cosh^2\left(X\right)}+\frac{2}{cosh^3\left(X\right)}\right]dt\right\} \quad (4.10)$$

where $\partial h_e = \frac{1}{H_1}\frac{\partial H_e(t)}{\partial t}$, $Y = \frac{H_{\max} - H_e}{2H_c}$, $X = \frac{H_{\min} - H_e}{2H_c}$, $t_{1,}$ is t_2 are the points at which the external field reaches its maximum and minimum, respectively.

We obtain the following expression for the total loss power (the sum of the loss powers in a superconductor and normal-metal) per length unit in a coated conductor:

$$\frac{P_{Htot}}{\left(\mu_0^2 d_m a^3/3\rho\right)H_1^2\omega^2} = p_H = F_h + c_h Q_h \ , \quad (4.11)$$

where $Q_h = 6\frac{\Delta h}{h_1^{\,2}}g\left(\Delta h\right)$, $c_h = \frac{\pi\rho}{\mu_0 a d_m \omega}$, $h_1 = \frac{H_1}{H_c}$.

Here losses are normalized to the eddy losses caused by the uniform magnetic field with the amplitude and frequency equaled to those of the main harmonic when a superconductor is absent.

4.1.2. Coated conductor with a transport current

Let us consider losses caused by a non-sinusoidal transport current $I(t)$ flowing in the y-direction without an external magnetic field. We study the case when the current maximum I_{max} and module of the current minimum I_{min} are less than the critical value $I_c = 2aJ_c$. It is assumed that the magnetic field produced by a current induced in the metal is negligible in comparison with the field from the current in the superconductor. Losses in the superconductor are given by Eq. (3.3). To calculate the eddy current loss power P_{ied} per

length unit, Eq. (4.8) is used where, at a decrease (increase) of the current from its maximum (minimum) till the minimum (maximum), the magnetic field is determined as [17]:

$$H_z(x,t) = \tilde{H}_z(x, I_{max}, I_c) - \tilde{H}_z(x, I_{max} - I(t), 2I_c) \tag{4.12}$$

$$H_z(x,t) = \tilde{H}_z(x, I_{min}, I_c) + \tilde{H}_z(x, I_{min} - I(t), 2I_c) \tag{4.13}$$

where $\tilde{H}_z(x, I, I_c) = \begin{cases} 0, & |x| < b_i \\ 2H_c \dfrac{x}{|x|} \operatorname{arctanh}\left[\dfrac{x^2 - b_i^2}{a^2 - b_i^2}\right]^{1/2}, & b_i < |x| < a \end{cases}$,

and $b_i = a\sqrt{1 - I^2 / I_c^2}$.

Using the approach developed in section 4.1.1 the total loss power per length unit of a coated conductor carrying a non-sinusoidal transport current is:

$$\frac{P_{Itot}}{\left(\mu_0^2 d_m a^3 / 2\rho\pi^3\right) I_1^2 \omega^2} = p_I = F_i + c_h Q_i(\Delta i) \ , \tag{4.14}$$

where $\Delta i = \dfrac{I_{\max} - I_{\min}}{2I_c}$, $Q_i(x) = q(x)/i_1^2$, $i_1 = I_1/I_c$,

$$F_i = \frac{1}{\omega}\left\{\int_{t_1}^{t_2} \partial i(t)^2 \, G(b_i)\, dt + \int_{t_2}^{2\pi/\omega + t_1} \partial i(t)^2 \, G(\tilde{b}_i)\, dt\right\},$$

$$G(x) = 1 - x - \sqrt{1 - x^2}\operatorname{Log}\left(\frac{1 + \sqrt{1 - x^2}}{x}\right) + \frac{1}{2}\left[\operatorname{Log}\left(\frac{1 + \sqrt{1 - x^2}}{x}\right)\right]^2,$$

$$b_i = \sqrt{1 - \left(\frac{I_{\max} - I(t)}{2I_c}\right)^2} \ , \ \tilde{b}_i = \sqrt{1 - \left(\frac{I_{\min} - I(t)}{2I_c}\right)^2} \ , \ \partial i(t) = \frac{1}{I_1}\frac{dI(t)}{dt}.$$

4.2 Results and discussion

In the case of a sinusoidal waveform ($H_e(t) = H_1 \sin(\omega t)$ or $I(t) = I_1 \sin(\omega t)$), the dependence of the functions F_h, F_i, Q_h and Q_i on the magnetic field and current has been analyzed in

[17,33]. Under non-sinusoidal conditions when $I(t)=I_1\sin(\omega t)+I_k\sin(k\omega t+\phi_k)$, the monotonic behavior of the waveform is observed at $I_k/I_1 < 1/k^2$. Losses in the normal metal also depend on a phase of the higher harmonic. Our calculation showed that the maximum of the losses is achieved at the same phases at which losses in a superconductor are maximal: $\phi_2 = 0$ for the second harmonic and $\phi_3 = \pi$ for the third one. At design of superconducting power devices, one should calculate AC losses for the worst case when the losses are maximal, therefore here we will analyze the cases of the second harmonic with $\phi_2 = 0$ and of the third harmonic with $\phi_3 = \pi$. The numerical integration and graphical presentation were carried out using Mathematica. For monotonic waveforms functions F_h, Q_h and Q_i , F_i are shown in Figs. 12 and 13, respectively. Note, that functions F_h and F_i characterizing the eddy losses as well as functions Q_h and Q_i corresponding to losses in superconductor which are independent of frequency of the main harmonic. Despite this fact the total losses in a coated conductor are frequency dependent: eddy current losses are proportional to ω^2 and losses in a superconductor ~ ω. Using our normalization it is clearly shown that the relative contribution of losses in a superconductor losses depend on the parameter c_h which is frequency dependent, $c_h \sim \frac{1}{\omega}$. Thus the relative contribution of AC losses in a superconductor is given by the inverse relation of the main harmonic frequency.

The influence of higher harmonics on losses in a superconducting strip in perpendicular magnetic field has been analyzed in chapter 3, where it was shown that the hysteresis losses per a current period are independent of frequency of the harmonics. These losses depend only on the maximum and minimum of the current or magnetic field. Figs.14 and 15 present the relative contribution $\delta P = \left(P - P_1\right)/P_1$ of higher harmonics to losses (here P_1 is losses caused by the main harmonic). The contribution is maximal at a low magnetic field and decreases when the field increases. For example at $\frac{\Delta H}{2H_1} = 0.05$ for the third harmonic, the contribution to AC losses achieves 20% in a superconductor and 35% in the normal metal parts (Fig 15, green line). At a high field when screen properties of a superconductor can be neglected, eddy

losses are determined as for a normal-metal strip in the uniform external non-sinusoidal field and the relative contribution of the k-th harmonic is given by $\delta P = k^2 H_k^2 / H_1^2$ and for the 5% third harmonic losses in the metal increase by 2% and in the superconductor – by 5%.

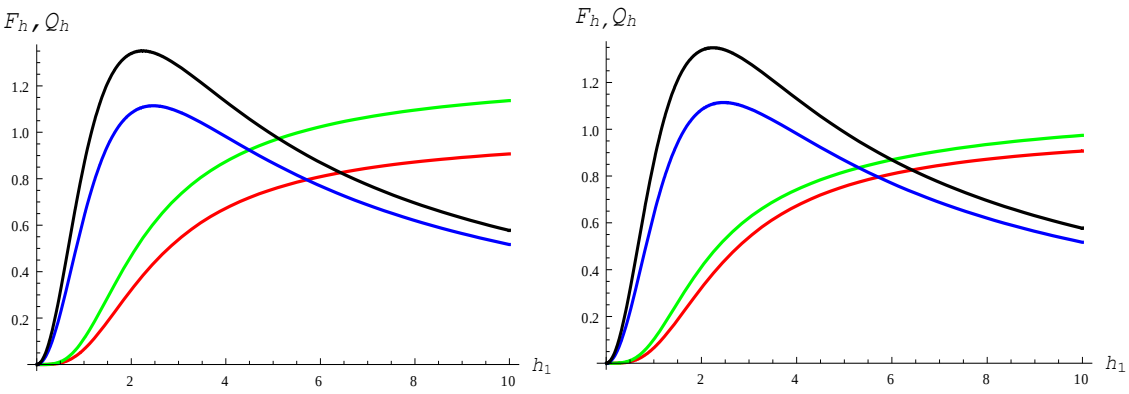

a) b)

Fig. 12 Dependences of the functions F_h and Q_h on amplitudes of two first harmonics: a) the case of the main and second harmonics at $\phi_2 = 0$ (blue, Q_h , and red, F_h , lines at H_2 =0; black, Q_h, and green, F_h, lines H_2 =0.25 H_1) and b) main and third harmonics at $\phi_3 = \pi$ (blue, Q_h , and red, F_h , lines at H_3 =0; black, Q_h, and green, F_h, lines at H_3 =0.1 H_1).

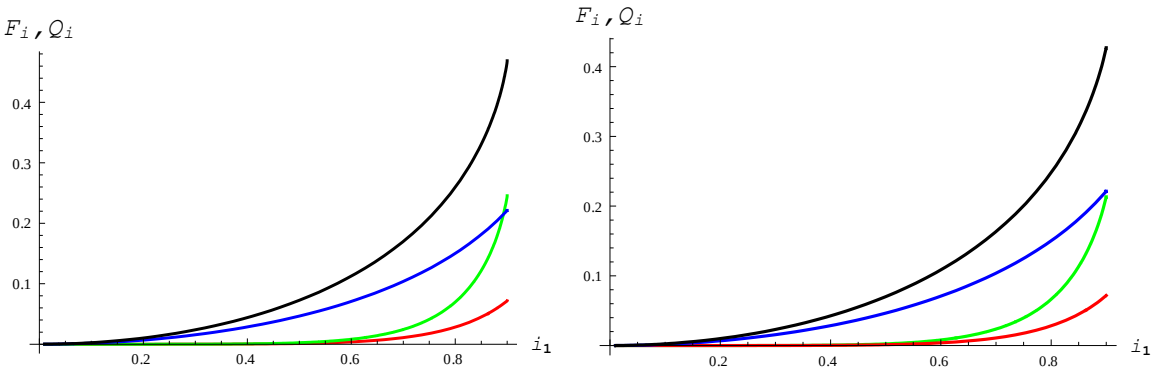

a) b)

Fig. 13 Dependences of the functions F_i and Q_i on amplitudes of two first harmonics: a) the main and second harmonics at $\phi_2 = 0$ (blue, Q_i, and red, F_i, lines at I_2 =0, black, Q_i, and green, F_i, lines at I_2 =0.25 I_1) and b) main and third harmonics at $\phi_3 = \pi$ (blue, Q_i, and red, F_i, lines at I_3 =0; black, Q_i, and green, F_i, lines at I_3 =0.1 I_1) .

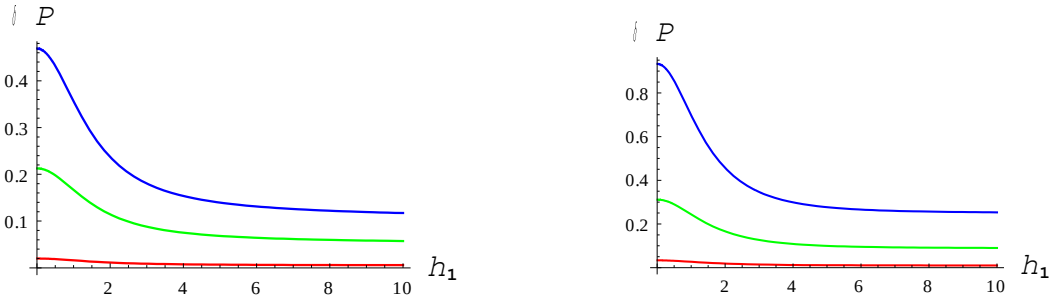

a) b)

Fig. 14 Relative contribution of the second harmonic of the magnetic field to losses in a superconductor (a) and normal-metal parts (b): blue line – H_2 =0.25 H_1; green – H_2 =0.15 H_1, red line – H_3 =0.05 H_1.

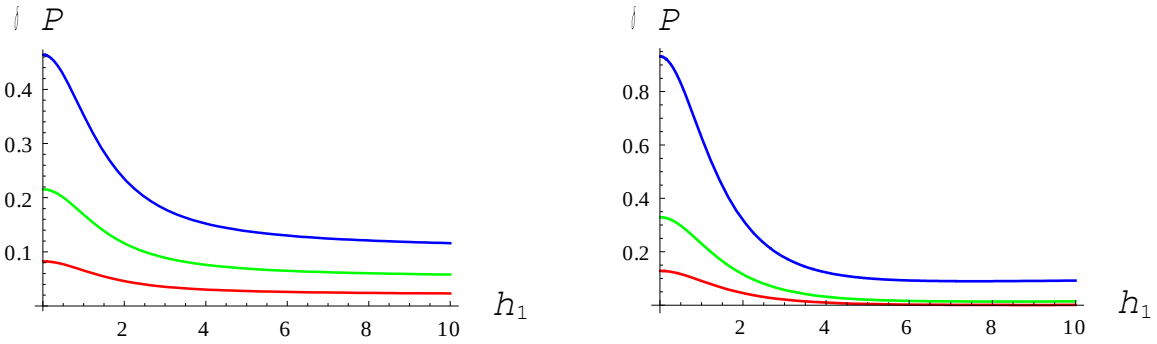

a) b)

Fig. 15 Relative contribution of the third harmonic of the magnetic field to losses in a superconductor (a) and normal-metal parts (b): blue line - H_3 =0.1 H_1; green – H_3 =0.05 H_1, red – H_3 =0.02 H_1

Fig. 18 shows the dependence of losses in a superconductor as function of third a) magnetic field and b) transport current harmonics, qualitatively similar behavior is expected for the second harmonics. Another dependence is obtained for a coated conductor with a transport current (Figs. 16, 17, 18b). At I_{max}-I_{min} <<I_c losses in a superconductor are determined by the expression similar to (3.4) with K = 4, where the magnetic field values are replaced by the corresponding currents. At $\Delta I/2I_1$ = 0.05 the losses increase also by about 20%. However, in contrast to the case of a magnetic field, the relative contribution increases with the current and achieves about 35% at $I \approx I_c$ (Fig. 17a, blue line). Qualitatively similar behavior is observed

for losses in the normal-metal parts: the relative contribution increases with the current (Figs. 16b and 17b).

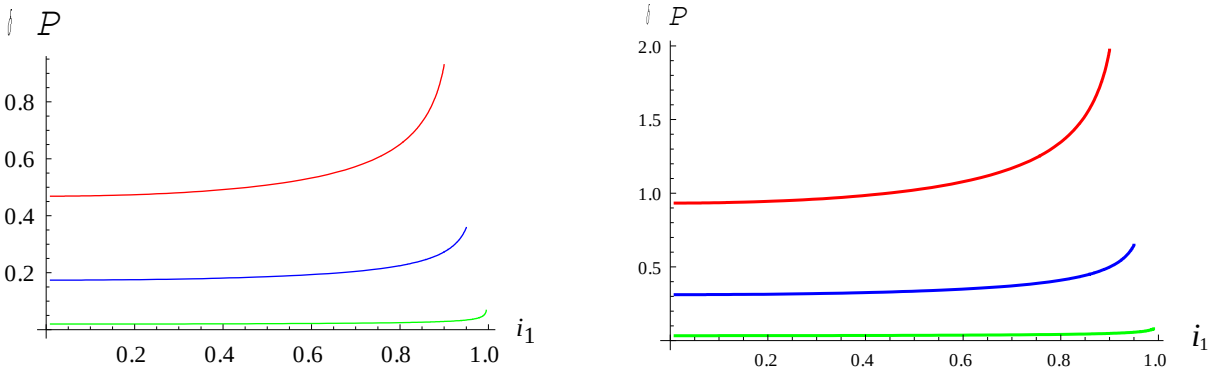

a) b)

Fig. 16 Relative contribution of the second current harmonic to losses in a superconductor (a) and normal-metal parts (b): red line – I_2 =0.25I_1 , blue line – I_2 =0.15I_1, green – I_2 =0.05I_1.

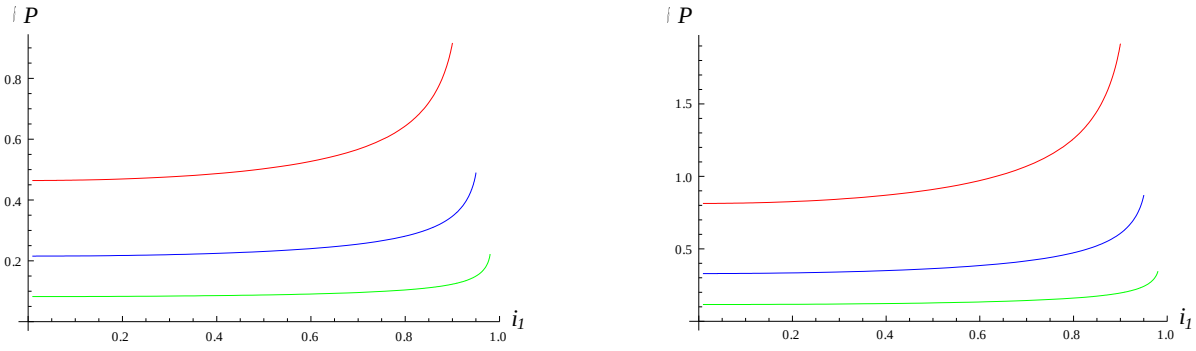

a) b)

Fig. 17 Relative contribution of the third current harmonic to losses in a superconductor (a) and normal-metal parts (b): red line - I_3 =0.1I_1 , blue line - I_3 =0.05I_1, green - I_3 =0.02I_1.

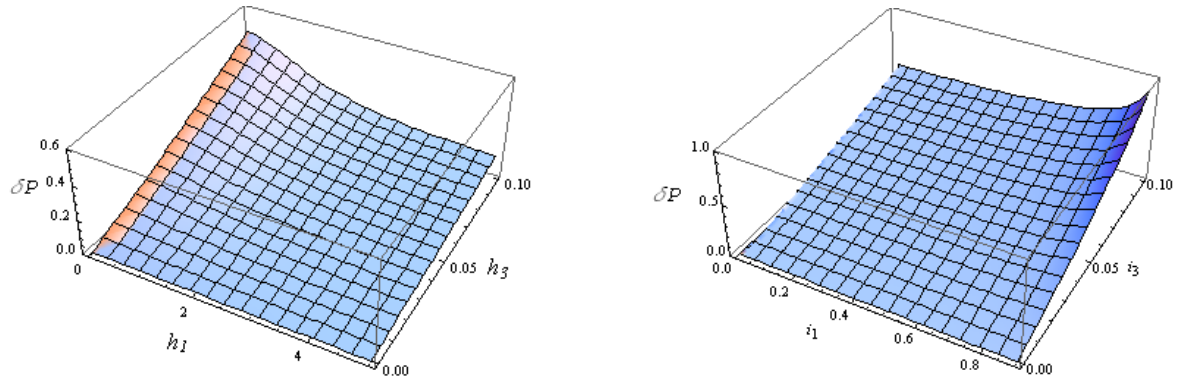

a) b)

Fig. 18 Relative contribution of higher harmonics to losses in the superconducting part of a coated conductor: a) contribution of the third magnetic field harmonic; b) contribution of the third current harmonic.

However, the relative contribution can be more substantial. For example, the 5%-third harmonic causes increase of eddy losses by about 35% at low currents and achieve about 80% at $I \approx I_c$ (Fig. 17b, blue line). At the same time losses in a superconductor increase by from 20% up to 45% (Fig. 17a, blue line).

The total losses in a coated conductor are determined by the sum of the losses in the superconducting and normal-metal strips. The relative contributions of these parts are determined by the ratio F_h and Q_h in case of the magnetic field and by the ratio F_i and Q_i for the current as well as by the constant c_h. At $h_1 << 1$ both functions, F_h and Q_h , are well fitted by power laws with exponents 4 and 2, respectively. At $h_1 >> 1$ Q_h decreases proportionally to $1/h_1$ while F_h tends to the limiting value $1+(kH_k/H_1)^2$. Thus, the relative contribution of eddy current losses to the total losses increases with the applied field (Fig. 12).

In spite of the fact that both functions F_i and Q_i increase (Fig. 13) with the current, the relative contribution of losses in a normal-metal strip to the total losses also increase. For example, for the 5% third harmonic the ratio $F_i / Q_i = 0.02$ at $i_1 = 0.2$ and this ratio increases up to about 0.6 at $i_1 = 0.9$.

Let us estimate the parameter c_h which is the same in the expressions for the total losses in both cases and depends on a frequency of the main harmonic and characteristics of the normal-metal strip (resistivity, thickness, and width) only. For a coated conductor without protective silver layer and stabilizer [33] the parameter c_h is evaluated as $(10^6\ s^{-1})/f$, for a conductor with the silver layer with thickness of ~2 μk [35] $c_h \approx (8\ 10^4\ s^{-1})/f$, for a well stabilized coated conductor with cooper stabilizer thickness of 100 μk [36] the parameter c_h is evaluated as $(1.6\ 10^3\ s^{-1})/f$. The estimations were done for the coated conductor with the width of 1 cm, the resistivity of a hastelloy-C substrate was taken $1.24\ 10^{-6}$ Ω m and resistivity of silver and cooper – $2\ 10^{-9}$ Ω m at 77 K.

One can see that the losses in a superconductor dominate in the two first conductor types till high frequencies of the order of 1 MHz. The losses in the normal-metal parts of a well stabilized coated conductor can be comparable or even dominate at electrotechnical

frequencies ~1 kHz (the range of frequency is used in special electric power systems such as airplanes, ships, etc.). At 50-60 Hz losses in the normal-metal parts will dominate in magnetic field $h_1 > 30$, e.i. when $\mu_0 H_1 > 0.1$ T at the typical value of $J_c = 10^4$ A/m ($\mu_0 H_c = 0.004$ T). This value is much less than the working magnetic fields in many power devices, for example, a working field in a generator is of the order of 1 T, and losses in the normal metal parts of a coated conductor dominate. In superconductor power cables the working fields are of the order of 0.03 T and the total losses are mainly determined by losses in a superconductor. Basing on the fact that AC loss values in a normal-metal parts can not exceed losses in a superconductor. Thus, AC loss values in a nominal regime of power devices imposes a restriction on the possible thickness of the stabilization layers.

For a coated conductor without a protective layer AC loss value in normal metal parts prevails losses in superconductor at the typical value of 10 T which is significantly higher than all the working magnetic fields in modern power devices.

4.3 Analytical approach for AC losses in striped coated conductors

A sufficiently AC-tolerant YBCO coated conductor can enable the fully superconducting version for motors and generators in which both the field and armature windings are superconducting [32]. From expressions (3.2) and (3.3) one can see that the value of hysteresis losses is proportional to the strip width in square.

The width of the developed coated conductor is 1 cm with plans to reduce it to 4 mm. When such a wide superconducting tape is exposed to time varying external field a large amount of heat is generated [5,37]. Thus, a significant reduction of hysteresis losses in coated conductors is a prerequisite for their use in AC power applications. It is also important for such a modification to be compatible with current techniques of manufacturing the coated conductors. To reduce hysteresis losses in tapes several millimeters wide, subdividing of the

tape into narrow parallel strips has been proposed [37]. The resulting conductor is a multifilamentary tape with parallel thin strips (filaments) separated by narrow gaps (Fig. 18). Let us consider losses caused by a perpendicular non-sinusoidal magnetic field in a striped coated conductor.

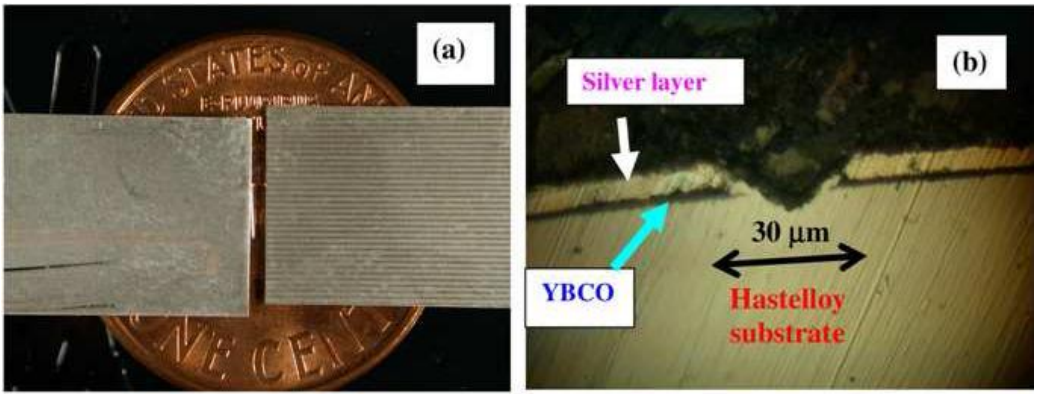

a) b)

Fig.19 a) One cm wide uniform coated conductor and 33-filament striated sample shown side by side the top visible layer is silver ; b) microphotograph of the cross-section of the striated sample in the groove area. The Hastelloy substrate, YBCO and silver layer are indicated.

It was shown [26] that the losses can be presented as a sum of the loss in a normal conducting substrate, the transverse coupling current loss and the loss in the filamentary strips. For a sufficiently high magnetic field these losses can be estimated separately assuming that the magnetic field equals the external one. To find the area of applicability of this approach we will use the solution obtained in the framework of the model of a thin strip [17]:

$$P_{xB} = P_0 g\left(h_1\right) \qquad (4.15)$$

where $P_0 = 4 f \mu_0 a^2 J_c H_1$.

At $h_1 >> 1$, $g\left(h_1\right) = 1 - 1.386 / h_1$. The last term, $-1.386 / h_1$ describes the decrease of losses during the lower field part of a period due to partial field penetration and also due to the difference among the local magnetic field to the external one. The term can be neglected at $h_1 \geq 15$ with an accuracy of 10%.

The value of J_c is typically of the order of 10^4 A/m for modern coated conductors [31]. Therefore $\mu_0 H_c \sim 4\times10^{-2}$ T and the approximation that the magnetic field equals the external one can be used for external magnetic fields with amplitudes higher than 0.6 T, typical for transformers, electrical motors and generators. Under this assumption, the coupling loss and loss in a substrate per length unit are given by the following expression

$$P_{ed} = \frac{K_1(f)H_1^2}{2}\left(1+\sum_{k\neq1} p_k h_k^2\right) \tag{4.16}$$

where $K_1(f)H_1^2/2$ is the eddy losses caused by the main harmonic, p_k characterize the dependence of the losses on frequency. Generalizing Eq. (44) from [5], we obtained for both losses $p_k = k^2$, for a strip $K_1 = \frac{2\mu_0^2 a^2 d_m \omega^2}{3\rho}$, while for the coupling losses per the length unite this coefficient is $a^2 L\omega^2 \big/ 3(N-1)R_g$, where L is the conductor length or the twisting step length, N is the number of filamentary strips, R_g is the resistance between two neighboring filaments. Losses in superconducting strips can be estimated using the results obtained above.

4.4. Power law superconducting strip

The results presented above have been obtained in the framework of the critical state model with the critical current density independent of a local magnetic field. A more realistic picture is given by the models based on a power law fitting of the voltage-current characteristic of a superconductor or/and taking into account the dependence of the critical current on a magnetic field. It was shown [6] that at high magnetic fields the loss values obtained for power-law dependence even with a high index of power (10-30) are markedly different from those given by the critical state models. Let us analyze the influence of higher harmonics on losses in a thin superconducting strip with the power-law relation between the sheet current

density J and electric field E and dependence of the critical current on a magnetic field according the Kim-Anderson model:

$$E = E_0\left(\frac{J}{J_c}\right)^n,\ J = J_c\frac{H_b}{|H|+H_b}, \tag{4.17}$$

where E_0 = 1 μV/cm is the electric field caused by the critical current density j_c and j_{c0} is its value at H = 0, H_b is a constant determined by the properties of the superconductor.

At high magnetic fields losses per unit of the strip length are

$$P = P_0\left[\frac{n}{4n+2}\left(\frac{\mu_0 w\omega H_1}{E_0}\right)^{1/n}\right]F, \tag{4.18}$$

$$F = \int_0^T \frac{\omega\left|\sum_{k=1} h_k k\cos\left(\omega kt+\phi_k\right)\right|^{1+1/n}}{1+h_b\left|\sum_{k=1} h_k \sin\left(\omega kt+\phi_k\right)\right|}dt\ ,$$

where $h_b = H_1/H_b$, $P_0 = 4f\mu_0 J_c a^2 H_1$ is the loss given by CSM in asymptotically high magnetic fields. The dependence of losses on the properties of a superconductor, n, E_0, H_b, has been investigated in [6] for a sinusoidal magnetic field.

The influence of higher harmonics on losses appears in the value F of the integral in (4.18). For a sinusoidal field (h_k = 0 for k >1) and at $n\to\infty$, h_b = 0, (the critical state model), this integral equals 4 and $P = P_0$. Let us analyze the value of F for two cases of a two-harmonic waveform: (a) k = 1, 2; (b) k = 1, 3. For practical applications it is important to determinate the maximum attainable values of AC losses. F has the maximum at ϕ_2 =0 in the case (a) and $\phi_3 = \pi$ in the case (b). The results of numerical integration are presented in Fig. 20 at h_b = 0 and (ϕ_2 =0, $\phi_3 = \pi$).

The value of F decreases with an increase of h_b approximately as $1/(1+0.85\ h_b)^{0.625}$ for both cases and increases with the amplitudes of higher harmonics proportional to $1+a_2h_2^{1.8}$ for the first case and $1+a_3h_3$ for the second case. The coefficients a_2 and a_3 depend on the power index n and parameter h_b. For h_b < 1 and n >10, within the accuracy of 10%, a_2 and a_3 can be

taken 1.3 and 0.9, respectively. The increase of n above 20 does not lead to a marked growth (the difference of the values of F at n = 20 and n = 40 is less than 2%).

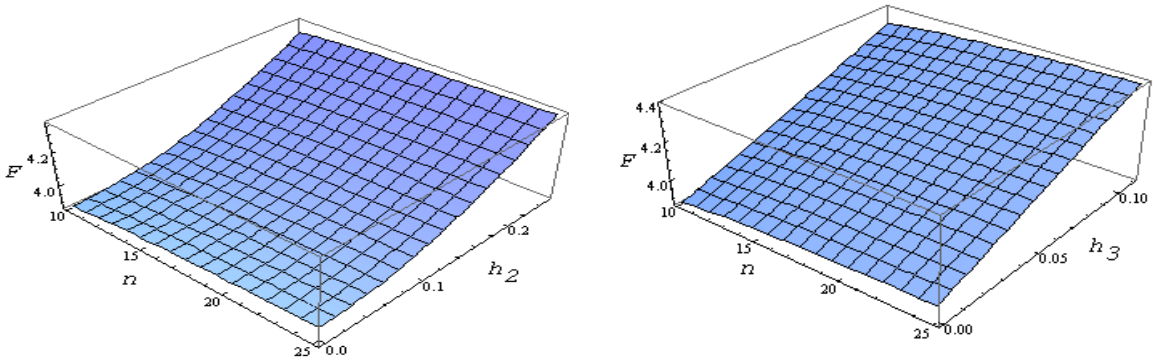

a) b)

Fig. 20 Dependence of F on n and a) h_2 for $H(t) = H_1 \sin(\omega t) + H_2 \sin(2\omega t)$, b) h_3 for $H(t) = H_1 \sin(\omega t) + H_3 \sin(3\omega t + \pi)$.

To determine the applicability of the approach developed in this section let us compare the asymptotic result for n>>1 and h_b =0 (Eqs. (4.18)), and analytical exact results obtained for CSM (see section 4.1.1). Fig. 21 shows that for the first harmonic amplitude higher than $15H_c$ one can use the approximation of asymptotic high magnetic field.

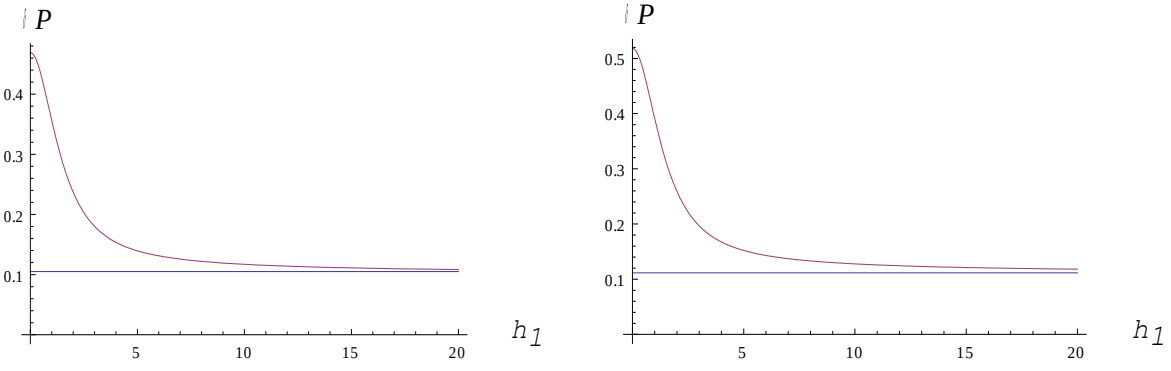

a) b)

Fig. 21 Relative contribution of higher harmonics to AC losses vs. amplitudes the main harmonics: a) the second harmonics; cyan line–CSM, blue - asymptotic high magnetic field approximation, b) the third harmonics: cyan line–CSM, blue - asymptotic high magnetic field approximation.

4.5 Summary

Our results show that higher harmonics can substantially change power losses in coated conductors, especially, in the conductors with a transport current. Thus, the 5% third current harmonic causes loss increase by 45% in the superconducting part of a coated conductor and by 80% in the normal-metal parts at a current close to the critical value. These peculiarities distinguish the behavior of coated conductors from that conventional ones when this harmonic increases losses by about 2%, only. So, it is very important to take into account higher harmonics at estimation of losses in coated conductors.

Note that approach of thin strips for estimation of losses can be applied also to superconducting films covered by stabilization (protective) layers, mono-filamentary thin tape based on YBCO and BSSCO ceramics.

5. Numerical analysis of AC losses in coated conductors

5.1 Introduction

In previous chapter we have analyzed AC losses in coated conductors in the framework of CSM and of the asymptotic high magnetic field approximation for a power law superconducting layer. It was shown that contribution of relative small higher harmonics to AC losses in coated conductors can achieve 110 % of losses caused by the main harmonic in a superconducting layer (Figs. 16, 17 and 18b) and 250% in a normal metal parts (Fig. 17b).

In this section we analyze influence of higher harmonics on losses in coated conductors simulated more real voltage-current characteristic – power law. Here the mathematical model and numerical algorithm are presented following [38].The algorithm was used to study the response of a coated conductor to pulse currents. We broadened and adopted the model and algorithm to calculation losses in power law coated conductors.

5.2 Mathematical Model

In the general case normal metal layers (substrate, protected and stabilized coverers) can be wider than a superconducting one. For loss calculation the coated conductors can be presented as a metal strip and a type II superconducting strip placed one on top of the other (Fig. 22) similarly to the model discussed in Section 4. The thickness of the metal strip is d_m and of the superconducting strip is d_{sc} and the half-width are a and a_{sc}, respectively. The length of both strip is the same, l, where $\{d_{sc}, d_m\} << a_{sc} < a << l$, and the approximation of infinitely long thin strips can be applied. In the framework of this approximation the magnetic field induced by a current in the conductor is perpendicular to the surface and is independent of the z-coordinate inside a strip. We shall consider losses in coated conductors for the following

cases: (i) a non-sinusoidal uniform magnetic field is applied perpendicular to the conductor wide surface (in the *z*-direction) without transport current and (ii) a non-sinusoidal transport current flows along the conductor in the *y*-direction without applied magnetic field. In both cases the electric field $\vec{E}$ and sheet current density $\vec{J}$ have only the *y*-components. In the thin strip approximation, the electric field is independent of the z- coordinate and is the same in the normal-metal and superconducting strips. The sheet current densities are various in these strips and distribution of the current between the strips is determined by their voltage-current characteristics.

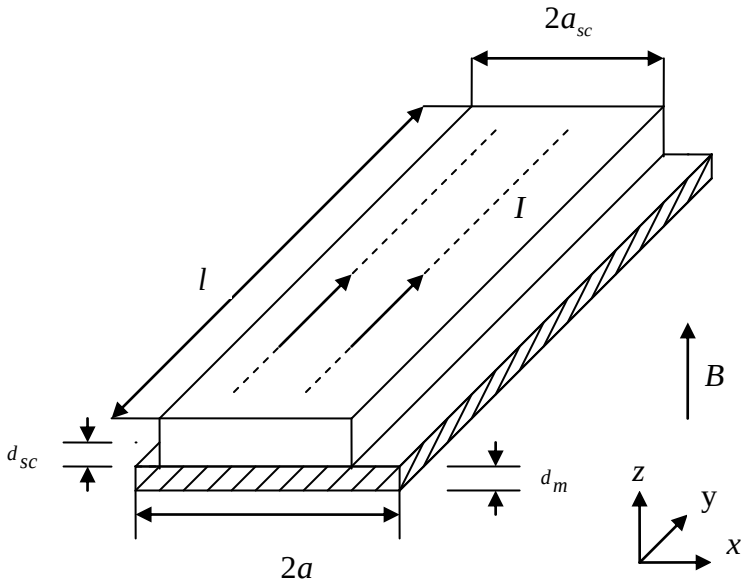

Fig. 22 Sketch of coated conductor simulated by two strips.

However, the results of experiments published in literature (see for example [39]) and of experiments performed at the Physics Department, BGU, showed that DC voltage-current characteristics of coated conductors are well fitted by a power law. Therefore, a local *E-J* relation can be written in the following form:

$$E = \begin{cases} \rho_m J / 2d_m & |a_{sc}| \le x \le |a| \\ E_0 \left(J / J_c \right)^n & x \le |a_{sc}| \end{cases} \qquad (5.1)$$

At z = 0, the z-component of the magnetic field is the sum of the external field $H_e(t)$ and field produced by a current:

$$H_z(x,t) = -\frac{1}{2\pi}\int_{-a}^{a}\frac{J(u,t)}{x-u}du + H_e(t). \tag{5.2}$$

The total current is given by

$$I(t) = \int_{-a}^{a} J(x,t)dx. \tag{5.3}$$

For the case (i): $I(t) = 0$, for the case (ii): $H_e(t) = 0$ and $I(t)$ equals the transport current $I_t(t)$.

By substitution of Eq. (5.2) into the Faraday law equation

$$\frac{\partial E}{\partial x} = \mu_0\frac{\partial H}{\partial t} \tag{5.4}$$

we obtain the following equation for the electric field

$$\frac{\partial E}{\partial x} = -\frac{\mu_0}{2\pi}\int_{-a}^{a}\frac{\partial J(u,t)}{\partial t}\frac{du}{x-u} + \mu_0\frac{dH_e(t)}{dt}. \tag{5.5}$$

In dimensionless units the last equation is rewritten as

$$\frac{\partial e}{\partial \zeta} = -\frac{\mu_0 a d_m}{\pi\tau\rho_m}\int_{-1}^{1}\frac{\partial e(u,\vartheta)}{\partial\vartheta}\frac{du}{\xi-u} + \frac{\mu_0 H_1 a}{E_0\tau}\frac{\partial h_k}{\partial\vartheta} \tag{5.6}$$

here $e = \frac{E}{E_0}$, $\xi = \frac{x}{a}$, $\vartheta = \frac{t}{\tau}$, $h_k = \frac{H_k}{H_1}$, and the normalization parameter E_0 can be arbitrarily chosen. The characteristic time is chosen by the following formula

$$\tau = \frac{\mu_0 a d_m}{\pi\rho_m}. \tag{5.7}$$

as a result Eq.(5.6) may be rewritten in the following form

$$\frac{\partial e}{\partial \zeta} = \int_{-1}^{1}\frac{\partial e(u,\vartheta)}{\partial\vartheta}\frac{du}{\zeta-u} + \eta\frac{\partial h_k}{\partial\vartheta},$$

where $\eta = \frac{H_1\pi\rho_m}{E_0 d_m}$.

5.3 Numerical algorithm

To develop a numerical algorithm we integrate equation (5.5) with respect to the *x*-coordinate substitute $E=\rho(x,J)J/2a$ where $\rho(x,J)$ is a nonlinear resistivity corresponding to the $E-J$ characteristics of a coated conductor and obtain

$$\rho(x,J)J/2d_m=-\frac{\mu_0 d_m}{\pi}\int_{-a}^{a}\frac{\partial J(u,t)}{\partial t}ln|x-u|du+\frac{\partial A}{\partial t}-C(t) \tag{5.8}$$

where $C(t)$ is unknown function of time and *A* is the vector potential of external magnetic field

The system of equations (5.2) and (5.5) determines both the current distribution in a conductor and the function $C(t)$ was solved numerically.

Let $\{x_i\}$, $i=0,.....N$ be an equidistant mesh on $[-a,a]$ with $\Delta=x_i-x_{i-1}$. We use piecewise-constant finite elements and approximate $J(x,t)$ by $\sum_{j=1}^{N}J_j(t)\delta_j(x)$ where

$$\delta_j(x)=\begin{cases}1 & x_{j-1}\le x\le x_j\\ 0 & \text{otherwise}\end{cases} \tag{5.9}$$

Multiplying equation (5.5) by $\delta_i(x)$ $i=0,...,N$ and integrating we obtain

$$M\frac{\partial \bar{J}}{\partial t}=\Delta\left(-\bar{b}\left(\bar{J},t\right)+\frac{\partial A}{\partial t}-C\bar{1}\right) \tag{5.10}$$

where

$\bar{b}_i\left(\bar{J},t\right)=\rho_i(J_i)J_i,\quad \rho_i(J_i)J=\rho(x_{i-1/2},J_i),\quad x_{i-1/2}=x_i-\Delta/2,\quad \bar{1}=(1,1.....1)^T$; .The integrals $M_{ij}=\frac{\mu_0 d_m}{\pi}\int_{-a}^{a}\int_{-a}^{a}\delta_j(x)\delta_i(y)\ln|x-y|dxdy$ can be found analytically

$M_{ij}=\frac{\mu_0 d_m\Delta^2}{\pi}\left(m_{|i-j|}+2\,ln\,\Delta\right)$ with

$$m_k=\begin{cases}-3 & k=0\\ -3+4\,ln\,2 & k=1\\ -3+(k+1)^2\,ln(k+1)-2k^2\,ln\,k+(k-1)^2\,ln(k-1) & k=2\end{cases}. \tag{5.11}$$

For each time moment we substitute $\frac{\partial \bar{J}}{\partial t} = \Delta M^{-1}\left(\bar{b}\left(\bar{J},t\right)+\frac{\partial A}{\partial t}-C\bar{1}\right)$ into the equation $\frac{\partial I}{\partial t} = \Delta\sum_{i=1}^{N}\frac{\partial J}{\partial t}$ obtained from Eq. (5.3) and find

$$C = \left(\sum_{j=1}^{N}\left(-M^{-1}\bar{b}\left(\bar{J},t\right)\right)_j + \frac{\partial A}{\partial t} - \frac{\partial I}{\partial t}\frac{1}{\Delta^2}\right) \Big/ \sum_{i,j=1}^{N} M_{ij}^{-1}. \qquad (5.12)$$

Now using standart routine for ordinary differential equations we can integrate over time the system

$\frac{\partial \bar{J}}{\partial t} = \Delta M^{-1}\left(-\bar{b}\left(\bar{J},t\right)+\frac{\partial A}{\partial t}-C\bar{1}\right)$ with zero initial conditions.

The value of AC losses per a period is calculated according to:

$$P_t = \int_0^T dt \int_{-a}^{a} \vec{E}\cdot\vec{J}\,dx \qquad (5.13)$$

Here P_t represents total AC losses per a period which is the sum of losses in normal and superconducting parts

In our algorithm we use a differential equation for calculation of AC losses:

$$\frac{dP_t}{dt} = \int_{-a}^{a} \vec{E}\cdot\vec{J}\,dx$$

with zero initial conditions.

The numerical algorithm was realized using “MatLab” and is given in dimension units. We can easily use it in dimensionless units by replacing the appropriate coefficients, for example a is replaced by 1.

In calculations we used the dimensionless units with the timescale τ chosen for a normal metal tape according to Eq. (5.6) and $\xi = x/a$. In these units, the resistivity of normal conducting parts near the conductor edges $\frac{|a_{sc}|}{a} < \xi \le 1$ is equal to unity. Our estimation for a well stabilized coated conductor showed that the power law characteristic for the central part $\xi \le \frac{|a_{sc}|}{a}$ containing the superconductor can be taken in the following dimensionless form:

$\tilde{\rho}(J) = 0.015|J / J_c|^{n-1}$. Calculations below were performed for dimensionless time τ estimated for the current frequency of 50 Hz.

5.4 Results and discussion

The numerical algorithm has been tested in comparison with the numerical and analytical results for a thin superconducting film described by CSM. At 400 steps through the conductor width, an error in loss determination is less than 1%. Below all the calculations were performed at step number of 400 with zero initial conditions. Our calculation show that the process steadies during the first period for $n = 4,10,25$ and losses per a period do not practically change from a period to period.

Results of the numerical calculations of relative contribution of higher harmonic to the total losses in coated conductors are presented in Figs. 23-26.

In both considered cases((i) a non-sinusoidal uniform magnetic field and (ii) a non-sinusoidal transport current) the relative contribution of higher harmonics increases with the harmonic amplitude (Figs. 23 and 24). The contribution increases also with the power index *n*. At *n* = 25 the results for the power law model and critical state model are about the same and can be about 10 times larger than in a normal metal (Fig. 23 b). The contribution can achieve about 110% of losses caused by the main harmonic. Simulation of a coated conductor by power law with low power index (*n* = 4) predicts losses (contribution) can achieve 45% of losses caused by the main harmonic (Fig. 23 b), up to 4 times higher than losses caused by the same harmonic in the normal metal (~11%).

The relative contribution increases with the main current harmonics (Figs. 25 a and 26 a) while decreases when the main magnetic field harmonics increase (Fig. 25 b and 26 b). Similar behavior of the relative contribution of higher harmonics was observed for superconducting strips considered in the frame of CSM in section 4.

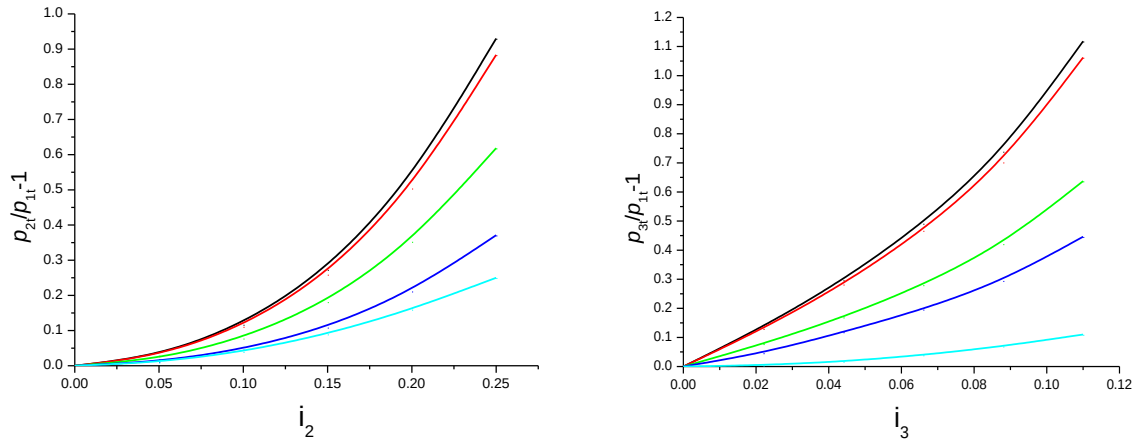

a) b)

Fig. 23 Numerical results of power law voltage –current characteristics (n = 10) for AC losses as function of higher harmonics; a) the second harmonics; b) - the third harmonics; Black line – critical state model; cyan line - normal metal; red, green, and blue lines – power law voltage-current characteristics with n = 25, 10, and 4, respectively.

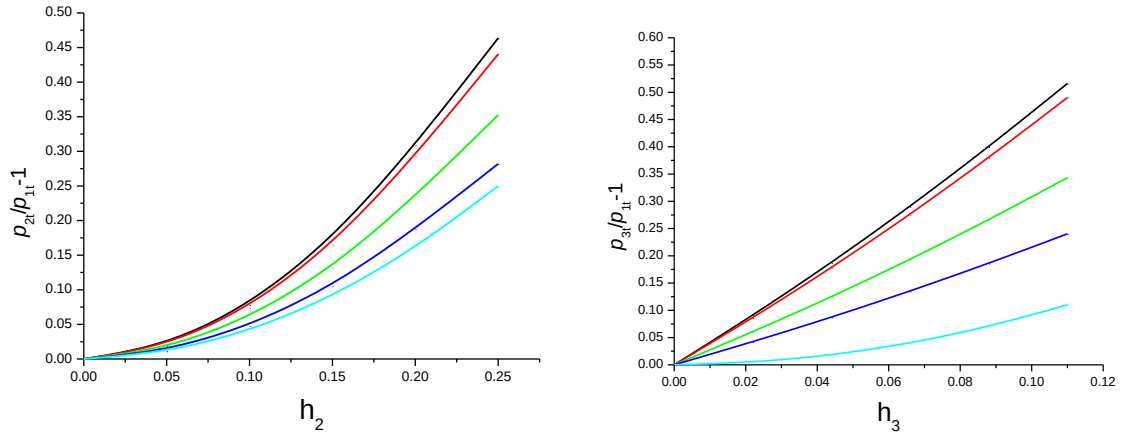

a) b)

Fig. 24 Numerical results of power law voltage –current characteristics (n = 10) for AC losses as function of higher harmonics a) second current harmonics b) second field harmonics; Black line – critical state model; cyan line - normal metal; red, green, and blue lines – power law voltage-current characteristics with n = 25, 10, and 4, respectively.

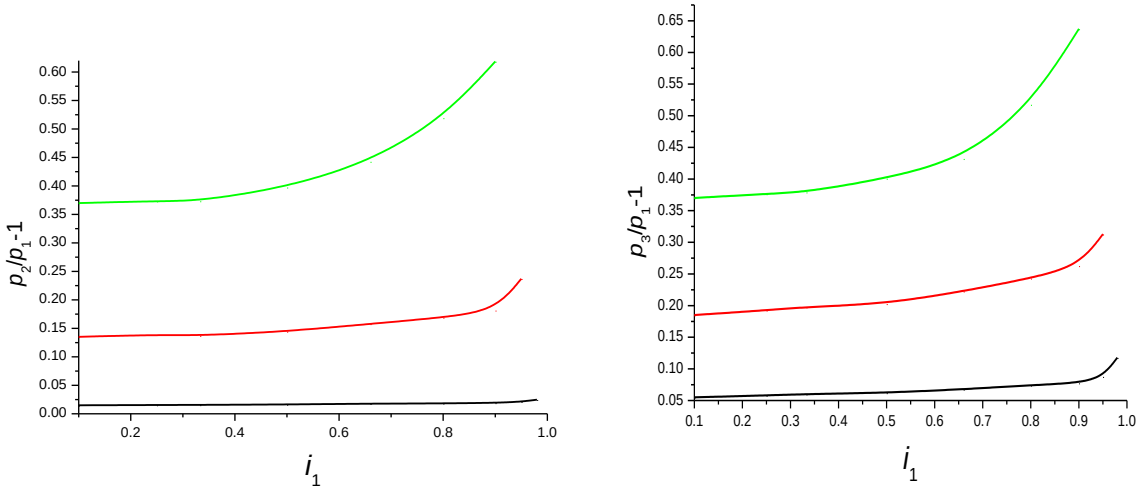

a) b)

Fig. 25 Relative contribution of the higher current harmonic to the total losses in a coated conductor described by a power law voltage-current characteristic a) the second harmonics; b) - the third harmonics;

green line-$h_2 = 0.25\ h_1$, red line- $h_2 = 0.15\ h_1$, black line- $h_2 = 0.05\ h_1$

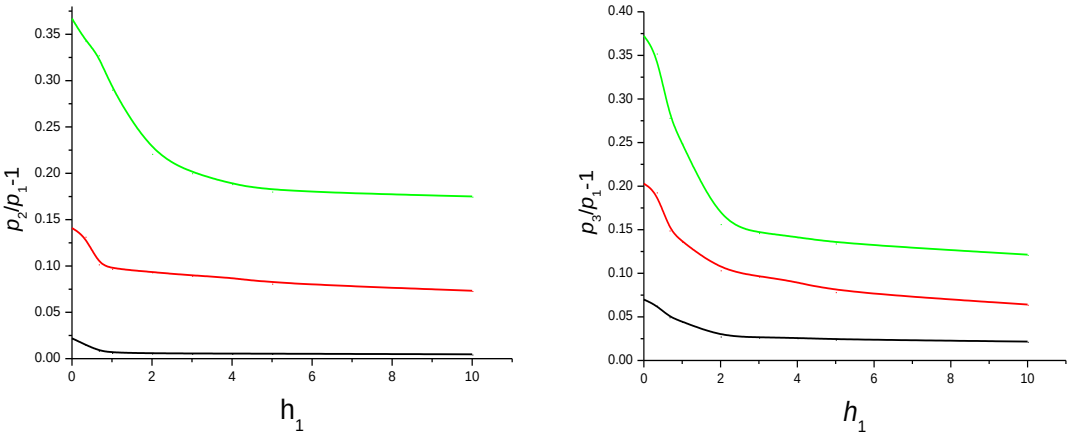

a) b)

Fig. 26 Relative contribution of the higher current harmonic to the total losses in a coated conductor described by a power law voltage-current characteristic a) the second harmonics; b) - the third harmonics;

green line-$h_3 = 0.1\ h_1$, red line- $h_3 = 0.05\ h_1$, black line- $h_3 = 0.02\ h_1$

5.5 Summary

The adopted algorithm for numerical calculation of AC losses in coated conductors gives well agreement with the analytical results obtained in the framework of the critical state model at the step number of 400 through the conductor width. As is expected for a high power index (n = 25) the analytical approach using CSM and numerical calculation within the power-law approximation give close results. The relative contribution of the third 10% harmonic can achieve up to 110% of losses caused by the main harmonic that is about ten times larger than losses caused by the same higher harmonic in the normal-metal conductor of the same form. Even at low power index (n = 4) the predicted losses are substantially higher than AC losses in normal metals: relative contribution can be 4 times higher and achieves 44% of main harmonic losses replace of 11%.

The relative contribution increases with the higher magnetic field and current harmonics as well as with the main current harmonics while decreases when the main field harmonics increase.

6. Conclusion

The behaviour of superconductors under non-sinusoidal conditions was investigated describing a superconductor by a nonlinear voltage-current characteristic. The main attention was given to analysis of the contribution of higher harmonics to AC losses in superconductors.

Analytical expressions were obtained for various configurations of superconductors such as: slab, thin strip, coated conductors in the framework the of critical state model as well as in the high magnetic field approximation for a power law superconductor. Analysis of losses in power law superconductors was carried out using MatLab software performing numerical solution of the integral equation.

The analysis shows that in devices with bulk superconductors, higher harmonics can substantially change losses. Thus, the 5% second harmonic can cause the loss increase by 20% in superconductors while by 1% in a normal metal. Moreover, the contribution of the higher harmonics depends on their phases: in a certain range of phases, the odd harmonics can even reduce AC losses. These peculiarities distinguish the behavior of superconducting devices from that of conventional ones. The increase of the amplitude of higher harmonics leads to the violation of the monotonic character of the waveform change from the minimum (maximum) to the maximum (minimum). Non-monotonic character of the waveforms of a current or a magnetic field influences AC losses only at very high amplitudes of higher harmonics.

Influence of higher harmonics losses in coated conductors is markedly stronger. Thus, the 5% third current harmonic causes loss increase by 45% in the superconducting part of a coated conductor and by 80% in the normal-metal parts at a current close to the critical value.

Numerical calculation of the total losses (sum of losses in superconducting and normal metal parts) in a coated conductor within the power-law approximation gives close results to ones obtained using the analytical approach for CSM at a high power index (n = 25), as is expected. The relative contribution increases with the higher magnetic field and current

harmonics as well as with the main current harmonics while decreases when the main field harmonics increase. The relative contribution of the third 10% harmonic to the total losses can achieve up to 110% of the losses caused by the main harmonic that is about ten times larger than losses caused by the same higher harmonic in the normal-metal conductor of the same form. Even at low power index (n = 4) the predicted losses are substantially higher than AC losses in normal metals: relative contribution can be 4 times higher and achieves 44% of main harmonic losses replace of 11%.

7. Bibliography

[1] W. J. Carr Jr., "AC loss and macroscopic theory of superconductors", New York: Taylor and Francis, 2nd ed, 2001.

[2] C. P. Bean, "Magnetization of High-Field Superconductors", *Rev. Mod. Phys.*, **36**, pp 31-39, 1964.

[3] Studies of high temperature superconductors, Ed. A. Narlikar, Vol. 32, "A.C. losses and flux pinning in high temperature superconductors", New York: Nova Science Publishers, 2000.

[4] E. Zeldov, John R. Clem, M. McElfresh, M. Darwin, "Magnetization and transport current in thin superconducting tapes", *Phys. Rev.*, **B 49**, pp 9802-9822, 1994.

[5] W. J. Carr Jr., "Loss in a striated coated conductor", *Supercond. Sci. Technol.*, **20**, pp. 168-175, 2007.

[6] V. Sokolovsky, V. Meerovich, "Analytical approximation for AC losses in thin power-law superconductors", *Supercond. Sci. Technol.*, **20**, pp. 875-879, 2007.

[7] P.W. Anderson, "Theory of flux creep in Hard Superconductors ", *Phys. Rev. Lett*., **9**, pp. 309-311, 1962.

[8] E.H. Brandt, "The flux line lattice in high T_C Superconductors", *Journal of alloys and Compounds*, **181**, pp 339-356, 1992.

[9] L.D. Landau, E.M. Lipshitz, " Statistical physics" , Moskva FizMatLit, 2001.

[10] J. Bardeen, M.J . Stephen, "Theory of the Motion of Vortices in Superconductors ", *Phys. Rev*., **140**, A1197-A1207, 1965.

[11] M.W. Coffey, J. R. Clem, "Unified theory of effects of vortex pinning and flux creep upon the rf surface impedance of type –II superconductors", *Phys. Rev. Lett*., **67**, pp. 386-389 1991

[12] C.P. Bean, "Magnetization of Hard Superconductors", *Phys. Rev. Lett*., **8**, pp. 250-252, 1962.

[13] L.D. Landau , E.M. Lipshitz, " Hydrodynamics" , Moskva, FizMatLit, 2001,

[14] L.D. Landau, E.M. Lipshitz, "Electrodynamics of continuous media" , Moskva, FizMatLit, 2001.

[15] E. H. Brandt, “Penetration of magnetic ac fields into type-II superconductor", *Phys Rev Lett.*, **67**, pp. 2219-2222, 1991.

[16] F. Gomory, "Characterization of high-temperature superconductors by AC susceptibility measurements", *Super. Sci. Technol*., **10**, pp. 523-542, 1997.

[17] E. H. Brandt, M. Indenbom, "Type-II-superconductor strip with current in a perpendicular magnetic field", *Phys. Rev.*, **B 48**, pp.12893-12906, 1993.

[18] W .T. Norris, "AC Losses in Superconductors "Calculation of hysteresis losses in hard superconductors carrying ac: isolated conductors and edges of thin sheets", *J. Phys D: Appl. Phys*, **3**, pp. 489-507, 1960.

[19] Y.B. Kimm, C.F. Hempstead, A.R. Strnad, "Critical Persistent Currents in Hard Superconductors " , *Phys.Rev.Lett.*, **9**, p.306, 1962.

[20] Y. Yeshurun, A.P. Malozemoff, A. Shaulov, "Magnetic relaxation in high temperature superconductors," *Rev. Mod. Phys.*, **68**, pp. 911-949, 1996.

[21] W.A. Fietz, W.W. Webb, " Hysteresis in superconducting alloys –Temperature and field dependence of dislocation pinning in niobium alloys", *Phys. Rev*. **178,** pp. 657-667, 1969.

[22] M. Xu, D. Shi, R.F. Fox, "Generalized critical state model for hard superconductors", *Phys. Rev*. **B42**, pp. 10773-10776, 1990.

[23] T. Matshushita, "Flux pinning in superconducting 123 materials", *Supercon. Sci. Technnol*., **13**, pp.730-737, 2000.

[24] A. Sanchez , C. Navau , "Magnetic properties of finite superconducting cylinders", *Phys. Rev*. **B64**, 214506, 2001.

[25] E.H. Brandt, "Superconductor disks and cylinders in an axial magnetic field", *Phys.Rev*. **B58**, pp. 6506-6522, 1998.

[26] V. Sokolovsky, V. Meerovich, S. Goren, G. Jung, "Analytical approach to AC loss in high-T_C superconductors", *Physica. C* **306**, pp. 154-162,1998.

[27] G. Blatter, M .V. Feigelman, V.B. Geshkenbein, A.I. Larkin, V.M. Vinokour, "Vortices in high-temperaturesuperconductors", *Rev. Mod. Phys.* **66** , pp. 1125-1388,1994.

[28] T.T.M. Palstra, B .Batlogg, R.B. van Dover, L.F. Schneemeyer, J.V. Waszcak, "Dissipative flux motion in high temperature superconductors", *Phys.Rev.* **B41**, pp. 6621-6632, 1990.

[29] E.H.Brandt, "Flux diffusion in high-*T*c superconductors" , *Z. Phys* **B80**, pp.167-175, 1990.

[30] M.V. Feigelman, V.B. Gashkenbein, A.I. Larkin, "Pinning and creep in hard superconductors," *Physica* **C 167**, pp.177-187, 1990.

[31] A. Sheth, H. Schmidt, V.Lasrado , "Review and evaluation of methods for application of epitaxial buffer and superconductor layers", *Appl. Supercon.* **6** , pp. 855-873, 1998.

[32] A.P. Malozemoff, "Progress in high temperature superconductor coated conductors and their applications", *Supercon. Sci. Technol*. **21**, 034005, 2008 (7p).

[33] K.–H. Muller, "AC power losses in flexible thick films superconducting tapes", *Physica* **C 281**, pp.1-10, 1997.

[34] K.–H. Muller, "AC losses in stacks and arrays of YBCO/hastelloy and monofilamentary Bi-2223/Ag tapes ", *Physica* **C 312,** pp.149-167, 1999.

[35] E. Martinez, L.A. Angurel, J. Pelegrin, Y.Y. Xie, V. Selvamanickam, "Thermal stability analysis of YBCO coated conductors subjected to over currents", *Supercon. Sci. Technol.* **23**, 025001, 2010 (8p).

[36] X. Wang, U.P. Trociewitz, J. Schwartz, "Self field quench behaviour of $YBa_2Cu_3O_{7-\delta}$ coated conductors with different stabilizers" , *Supercon. Sci.Technol*. **22**, 085005, 2009 (13p).

[37] J.Carr , " AC loss and Macroscopic Theory of Superconductors", Taylor and Francis , New York , 2001.

[38] V. Meerovich, V. Sokolovsky, L. Prigozhin, D. Rozman, "Dynamic response of HTS composite tapes to pulsed currents", *Super. Sci. Technol.* **19**, pp.267-275, 2006.

[39] J.S. Lamas, C.A. Baldan, C.Y. Shique, A. Silhanek, V. Molchakov, "Electrical and Magnetic Characterization of BSSCO and YBCO HTS Tapes for Fault Current Limiter Application", conference report at ASC-2010.

תקציר

הפסדי אנרגיה במוליכי-על מאפיין את תכונותיהם הפיסיקליות כגון (התנועה המיקרוסקופית של מערבולות אבריקוסוב, מופע של סריג ערבול וכדומה...), כמו כן לקבוע טווחים של הזרמים והשדות המגנטיים הנמדדים להתקני מוליכות על, ההספק הנדרש מהציוד הקריוגני והרווח הכלכלי.הדרכים למדידת הפסדי אנרגיה במוליכי-על מתבססים על משוואות מקסוול לא ליניאריות כאשר מוליך-על מתואר בעזרת תווך עם אופיין לא ליניארי בין המתח-לזרם, תלוי בטמפרטורה ובשדה המגנטי המקומי. הרבה מחקרים מוקדשים לנושא של הפסדי אנרגיה במוליכי-על מצורות שונות (תיל, סרט דק, מוליך מצופה) תחת תנאים שונים.

המטרה העיקרית של התיזה הזאת היא שקול של איבודי אנרגיה במוליכי-על ובמוליכים מצופים תחת תנאים לא-סינוסואידליים.

במסגרת המודל המצב הקריטי ותחת הקרוב של השדה המגנטי הגבוה למוליכי על לא- ליניאריים נתקבלו ביטויים אנליטיים עבור תצורות שונות של מוליכי- על כגון : חומרים צברים, פסים דקים, מוליכים מצופים.

ניתוח איבודי אנרגיה במוליכי על לא ליניאריים נעשה באמצעות תוכנת Matlab כאשר בוצע פתרון נומרי של משוואות דיפרנציאליות. הניתוח מראה כי בהתקנים של מוליכי-על צברים הרמוניות נוספות יכולים לשנות באופן ניכר את ההפסדים.לפיכך תוספת של 5% בהרמוניה שנייה גורם לעלייה בהפסדים ב 20% במוליכי-על לעומת עלייה של 1% במוליך רגיל. הייחודיות הנ"ל של מוליכי-על מבדילה בין מוליכי-על למוליכים רגילים.

השפעה של מוליכים מצופים ניכרת עוד יותר. לפיכך תוספת של 5% בהרמוניה שלישית גורמת לעלייה בהפסדים ב-45%

בחלקים העל מוליכים ו-80% בחלקים הנורמאלים.

חשוב נומרי של הפסדי אנרגיה כוללים (הסכום של הפסדים בחלקי ם העל-מוליכים ובחלקים הנורמאלים) במוליכים מצופים תחת ההנחה של power-law הראה כי התרומה היחסית של הרמוניות נוספות להפסדים גדלה עם המשרעת שלהם. התרומה היחסית של 10% בהרמוניה שלישית יכולה לגרום לעלייה ב-110% מההפסדים הנגרמים מההרמוניה הראשית שזה פי 10 פעמים מהאיבודים הנגרמים ע"י אותה הרמוניה למוליך רגיל מאותה צורה.

אפילו בחזקות נמוכות (n=4) ההפסדים הנצפים גבוהים באופן ניכר מההפסדים במוליך רגיל: התרומה היחסית היא פי 4 וגורמת לעלייה ב-45%.

נושא החיבור: איבודי אנרגיה במוליכי על תחת שדות מגנטיים וזרמים חשמליים לא סינוסידליים

חיבור לשם קבלת תואר "מגיסטר"

בפקולטה למדעי הטבע

מאת ספקטור מרט

שם המנחה ד"ר סוקולובסקי ולדימיר

שם המנחה פרופ' ראובן שוקר

המחלקה לפיסיקה

הפקולטה למדעי הטבע

אוניברסיטת בן גוריון בנגב

חתימת המחבר	תאריך
חתימת המנחה	תאריך
חתימת המנחה	תאריך
אישור יו"ר ועדה מחלקתית	תאריך